Integrated Master in Environmental Engineering

Structured membranes for water desalination and purification

Master Thesis

Of

Patrícia Maria Rodrigues dos Reis Fernandes Lopes

Dissertation

Developed at

Laboratory of Catalysis and Materials (LCM)

LABORATÓRIO ASSOCIADO
LSRE LABORATORY OF SEPARATION AND REACTION ENGINEERING
Laboratório de catálise e materiais lcm
ASSOCIATE LABORATORY

U.PORTO
FEUP FACULDADE DE ENGENHARIA
UNIVERSIDADE DO PORTO

Supervisors:
Adrián Manuel Tavares da Silva
Sergio Morales Torres
José Luís Cabral da Conceição Figueiredo

Department of Chemical Engineering

February 2015

Acknowledgments

This limited space, surely, does not allow me to thank, as it should, to all the people who, throughout my academic route helped me directly or indirectly to fulfill my goals. Thus, I just leave a few words of recognition.

Firstly, I would like to express my gratitude to Doctor Sergio Morales Torres (Postdoctoral Researcher in FEUP), for his guidance and unconditional support that raised my scientific knowledge, certainly encourage my desire to want to know more and to do better. Thank you for the professionalism, the total availability and joy that always revealed to me. Surely, his knowledge was crucial for this Master thesis and that allowed me to have motivation each single day.

I am also grateful to my supervisor, Doctor Adrián Manuel Tavares da Silva, for his sympathy, all useful assertive recommendations as well for the opportunity and privilege to participate in this project and perform my Master Thesis.

I also would like to thank to Professor José Luís Figueiredo, director of LCM, for given me the opportunity to work in this laboratory, which contributed greatly to the academic enrichment.

Thanks to all the team of LCM, for providing the necessary conditions for the development of my thesis and for allowing my integration into this Research Group, with a huge sense of satisfaction companionship and help, especially to Tânia L. dos Santos Silva and Carla M. Pires Esteves.

I would like to express my huge gratefulness to my mother for always believing in me, making possible to complete this stage of my life, the end of a new beginning. I hope this step, I finish now, can in some way, give back and make up for all support.

Financial support for this work was provided by projects PTDC/AAC-AMB/122312/2010 co-financed by FCT (Fundação para a Ciência e a Tecnologia) and FEDER (Fundo Europeu de Desenvolvimento Regional) through Programme COMPETE (FCOMP-01-0124-FEDER-019503). This work was also partially co-financed by FCT and FEDER through project PEst-C/EQB/LA0020/2013 (COMPETE), and by QREN, ON2 (Programa Operacional do Norte) and FEDER through project NORTE-07-0162-FEDER-000050. Technical assistance by Dr. Carlos Sá and CEMUP team with SEM analysis is gratefully acknowledged

Resumo

O atual crescimento populacional e o aquecimento global estão fortemente envolvidas na origem da ausência de água potável em cerca de metade da população mundial. Como mais de 97 % da água no planeta é proveniente do mar, as tecnologias de dessalinização têm um grande potencial para a procura e conservação da água potável. A osmose direta (*forward osmosis* - FO) tem sido alvo de atenção no tratamento de águas residuais e na dessalinização de água do mar. Este processo consiste no transporte, através de uma membrana semipermeável, de água a partir de uma solução menos concentrada para outra mais concentrada, devido apenas à diferença da concentração entre ambas as soluções. Para que este processo seja aplicado com sucesso na dessalinização de água do mar são necessárias algumas melhorias relacionadas com condições de operação e propriedades das membranas utilizadas.

Assim, no âmbito do presente trabalho, prepararam-se membranas com compósito de película fina (*thin-film composite* - TFC) usando diferentes membranas comerciais como suporte, denominadas poliamida (PA), poliestersufona (PES), acetato de celulose (CA) e mistura de celulose éster (MCE). A textura e as propriedades químicas de todas as membranas foram analisadas por diferentes técnicas e o seu desempenho foi avaliado em FO com água destilada e salgada (0.6M NaCl) como soluções de alimentação e permeado, respetivamente. A membrana de PA-TFC apresentou o melhor desempenho, com fluxo de água (J_w) = 10.7 L h^{-1} m^{-2}, fluxo inverso de soluto (J_s) = 36 g h^{-1} m^{-2} e 99.98 % de rejeição de sal. Após a seleção de PA-TFC como melhor membrana, o processo de FO foi otimizado alterando diferentes parâmetros de operação tais como configuração da célula onde é colocada a membrana, velocidades de recirculação das soluções, tipo e concentração de solução permeado e, ainda, orientação da membrana. Assim, as condições para o desempenho da membrana PA-TFC foram otimizadas, obtendo-se os valores de J_w = 23.7 L h^{-1} m^{-2}, J_s = 124 g h^{-1} m^{-2} e 99.36 % de rejeição de sal, utilizando um caudal de recirculação de 17 mL min^{-1} para ambas as soluções, a configuração de célula designada como W, utilizando a camada ativa voltada para o permeado (ALDS - *active layer faced to the draw solution*) e com uma solução de permeado 5.0 M de concentração em NaCl. Por fim, um ensaio de dessalinização de água do mar através de FO com as melhores condições de operação e a melhor membrana, utilizando uma amostra real recolhida na costa de Leça de Palmeira (Portugal) como solução de alimentação. Após 2h, com a membrana de PA-TFC nas condições otimizadas obteve-se J_w = 13.7 L h^{-1} m^{-2}, no entanto verificou-se alguma diminuição do desempenho por *fouling* na membrana. Portanto, a dessalinização de água do mar é possível através de FO, embora seja importante produzir novas membranas com maior resistência ao *fouling* para prolongar a vida útil da membrana e a sua performance.

***Palavras Chave**: osmose direta; membranas de TFC; caudal de recirculação; configurações de células, solução permeado.*

Abstract

As a consequence of the exponential population growth and global warming, half of the world's population suffers from water shortages. The number of people affected by this problem is expected to become even more critical over the next 25 years and the search for clean water and renewable energy being two major concerns worldwide. With this dramatic scenario, innovation and implementation of novel technologies that not only provide increased sources of clean water, but also optimize energy efficiency are mandatory. Since more than 97 % of the water in the world is seawater, desalination technologies have a great potential to overcome the fresh water crisis, particularly in coastal areas. Forward osmosis (FO) has attracted growing interest in wastewater treatment and seawater desalination, because water is selectively transported across a semipermeable membrane from one solution to another of higher concentration, and the process is solely based on the difference in the chemical potential (concentration) of both solutions. To be successfully applied for seawater desalination, FO needs some improvements regarding the operating conditions and membrane properties.

Thus, thin-film composite (TFC) membranes were prepared by the interfacial polymerization method using different hydrophilic commercial membranes as supports, namely polyamide (PA), polyethersulfone (PES), cellulose acetate (CA) and mixed cellulose ester (MCE). The textural and chemical properties of all membranes were analyzed by different techniques and their performances were firstly assessed in the filtration of deionized (DI) water. Finally, TFC membranes were tested in FO with DI water and salty (0.6 M NaCl) water, as feed and draw solutions, respectively. The PA-TFC membrane presented the best performance with a water flux (J_w) = 10.7 L h^{-1} m^{-2}, a reverse solute flux (J_s) = 36 g h^{-1} m^{-2} and 99.98 % of ions rejection. Then, the FO process was optimized for this PA-TFC membrane, by studying different operating parameters such as membrane module configuration, solutions flow rate, type and concentration of the draw solution and membrane orientation. Thus, the performance of PA-TFC was enhanced, namely J_w = 23.7 L h^{-1} m^{-2}, J_s = 124 g h^{-1} m^{-2} and 99.36 % of ions rejection being reached with 17 mL min^{-1} of draw and feed flow rates, using a W-cell configuration, an ALDS orientation and a 5.0 M concentration of NaCl, as draw solution. Finally, seawater desalination driven by FO was carried out with the best operating conditions by using real seawater (collected in the costal area of Leça de Palmeira – Portugal) as feed solution. PA-TFC was active under these conditions optimized with a J_w = 13.7 L h^{-1} m^{-2} after 2 h, although certain fouling was also observed. Therefore, seawater desalination is possible by FO although new membranes highly resistant to fouling are needed to increase the membrane lifetime and performance.

***Keywords**: forward osmosis; TFC membranes; flow rate, membrane module configuration; draw solution.*

Table of Contents

List of Tables

List of Figures

Abbreviations

AL	Active layer
ALDS	Active layer faced to the draw solution
ALFS	Active layer faced to the feed solution
CA	Cellulose acetate
CDI	Capacitive deionization
CEOP	Cake-enhanced osmotic pressure
CNTs	Carbon nanotubes
CP	Concentration polarization
CTA	Cellulose triacetate
DI	Deionized water
DS	Draw solution
ECP	External concentration polarization
ED	Electrodialysis
FCT	Fundação para a Ciência e a Tecnologia
FD	Freeze desalination
FEUP	Faculdade de Engenharia da Universidade do Porto
FO	Forward osmosis
GO	Graphene oxide
HTI	Hydration technology innovations
i	Van't Hoff factor
ICP	Internal concentration polarization
IP	Interfacial polymerization
IPA	Isopropyl alcohol
LCM	Laboratory of Catalysis and Materials
LSRE	Laboratory of Separation and Reaction Engineering
MCE	Mixed cellulose ester
MEF	Multi-effect distillation
MPD	1,3 – phenylendiamine
MSF	Multi-stage flash distillation
NF	Nanofiltration
PA	Polyamide
PAH	Polyallylamine hydrochloride
PAI	Polyamide–imide
PAN	Polyacrylonitrile
PBI	Polybenzimidazole
PEI	Polyethyleneimine
PES	Polyethersulfone

PET	Polyethylene terephthalate
PS	Polysulfone
PSS	Polystyrene sulfonate
PVP	Polyvinylpyrrolidone
RO	Reverse osmosis
SL	Support layer
TDS	Total dissolved solids
TFC	Thin-film composite
TMC	1,3,5 – benzenetricarbonyl trichloride
TMP	Trans-membrane pressure
UF	Ultrafiltration

Nomenclature

ε	porosity	%
θ	contact angle	°
ρ_{IPA}	density of isopropyl alcohol	g cm^{-3}
ρ_p	density of polymer	g cm^{-3}
A	area	m^2
C_f	feed concentration	g L^{-1}
C_d	draw concentration	g L^{-1}
C_s	solute concentration	g L^{-1}
C_t	salt concentration at time t	g L^{-1}
d_{pore}	pore diameter	µm
J_s	reverse solute flux	g h^{-1} m^{-2}
J_w	water flux	L h^{-1} m^{-2}
m_d	weight of the dry membrane	g
m_w	weight of the wet membrane	g
M_w	molecular weight	g mol^{-1}
Q_{draw}	draw flow rate	mL min^{-1}
Q_{feed}	feed flow rate	mL min^{-1}
R	gas constant	L atm mol^{-1} K^{-1}
S_{BET}	surface area	m^2 g^{-1}
t	time	h
T	temperature	K
V	volume	m^3
V_p	volume of N_2 adsorbed	cm^3 g^{-1}
π	osmotic pressure	atm

1 Introduction

1.1 Introduction to the work plan

The search for clean water and renewable energy, as consequence of the exponential population growth, urbanization, the global warming and the depletion of fossil fuels, have become two of the major concerns in the globe. In the past century, the demand for clean water has increased, reaching and exceeding the limits of renewable water resources in areas such as the Middle East, North Africa and China [1].

Fresh and potable water is an essential human need and the scarcity of pure water is only expected to become even more critical in the next decades. In the current scenario of global water crisis, innovative and novel technologies that not only provide increased clean water production, but also optimum energy efficiency, are required [2]. In this way, many engineers and researchers have been dealing with strategies to treat polluted water, while others try to find alternative sources.

Since more than 97 % of the water in the world is seawater, desalination technologies have the potential to solve the fresh water crisis, particularly in coastal areas. Since the 1960's, desalination is becoming an attractive method to produce high quality water for both industrial and domestic usages. This technology holds great promise to reduce water scarcity in arid and densely populated regions of the world. In general, the desalination process requires either a thermal phase change (e.g., multi-effect distillation and multi-stage flash distillation) or membrane process separation (e.g, nanofiltration –NF–, ultrafiltration –UF-, reverse osmosis - RO- and forward osmosis –FO [3, 4]). In fact, RO is nowadays the established membrane technology at large scale, where dissolved solids present in the feed supply are concentrated to produce the rejected (clean water) concentrate stream. Therefore, RO requires high pressures to overcome the osmotic pressure and to drive the water from the saline to the freshwater side of the membrane, which have associated a high energetic cost and a short membrane lifetime by fouling. In this way, alternative methods for water purification and desalination, which lead to a less expensive and easy to operate process are strongly mandatory.

In the past decade, FO has attracted growing interest in wastewater treatment, seawater desalination and power generation [5]. FO is an osmotically driven membrane process that takes advantage of the osmotic pressure gradient to drive water across the semipermeable membrane from the feed solution side to the draw side. Due to the zero or very low hydraulic pressure on the process, FO has quite potential advantages (e.g., less energy input, lower fouling tendency, easier fouling removal and higher water recovery) over pressure-driven processes like RO. The

critical challenges in FO are currently focused in reducing the concentration polarization, membrane fouling, reverse solute diffusion, by enhancing the membrane and draw solute design [6].

Therefore, a functional FO process requires an easily recoverable draw solution (capable of generating high osmotic pressures) as well as a highly productive and selective membrane. Ideally, an efficient ultrafast permeation membrane should be as thin as possible to maximize the permeance, robust enough to withstand the applied pressure and should have a narrow distribution of pore size for excellent salt rejection [2, 7]. The membranes most widely used are thin-film composite (TFC) membranes and an asymmetric cellulose acetate (CA) membrane specifically designed by Hydration Technology Innovations (HTI) for RO. The hydrophilic nature of CA favours the proper wetting in comparison with hydrophobic membranes. Even so, the low water flux and high salt flux still observed for CA membranes due to the relatively poor water permeability and selectivity, have limited their application in FO [8].

In this thesis, different hydrophilic commercial membranes were used as supports to prepare TFC membranes. The performance of the commercial and TFC membranes was firstly assessed in the filtration of deionized (DI) water and then, the TFC membranes were tested in FO of salty water. The TFC membrane with the best performance was selected for FO experiments and the FO process was optimized by varying different operating parameters such as, feed and draw flux rates, membrane module configuration, membrane orientation, type and concentration of the draw solution.

1.2 Presentation of the Research Unit

The Laboratory of Catalysis and Materials (LCM) in partnership with the Laboratory of Separation and Reaction Engineering (LSRE), became a national Associate Laboratory in 2004, in recognition of the capacity of the two units to cooperate in a stable, competent and effective way in the prosecution of specific objectives of the National Scientific and Technological Policy. The Associate Laboratory is based in the Chemical Engineering Department of the Faculty of Engineering of University of Porto (FEUP), with two external Poles at Instituto Politécnico de Bragança and Instituto Politécnico de Leiria. FEUP is a public institution of higher education with financial autonomy and the largest Faculty of the University of Porto.

The present work was performed in the framework of a LCM research topic (development of nanostructured materials) and under financial support of a FCT project (PTDC/AAC-AMB/122312/2010). The work was carried out in the LCM laboratories located in the Department of Chemical Engineering/FEUP (E-301, E-302A and E-303). The most relevant equipments used in the present work were a stirred filtration cell, a prototype for the FO

experiments, an optical tensiometer (Attension mod. Theta) and an ion chromatograph (Metrohm 881 Compact IC with sequential suppression).

1.3 Structure of the thesis

The present MSc thesis is divided into six chapters:

(i) The first chapter contextualizes the problem that is under investigation in this work and regards the main points discussed throughout the Thesis.

(ii) The state of art is presented in the second chapter, besides the theoretical fundamentals of the methods applied.

(iii) The detailed description of the membranes prepared in this study as well as the characterizations performed and experimental details of the FO process are presented in the third chapter.

(iv) The results obtained during the project and their corresponding discussion are shown in the fourth chapter.

(v) The main conclusions resulting from this work are presented in chapter five.

(vi) The limitations encountered while performing the work are registered in the last chapter, together with some suggestions for future work.

2 State of the art, motivation and objectives

2.1 Forward osmosis as a desalination process

Water resources are quickly being exhausted and just 3 % of all water sources are potable. About 25 % of world's population does not have access to satisfactory quality and quantity of freshwater. More than 80 countries have serious water problems and even countries that do not still face the problem of freshwater scarcity may have to be aware in a near future [3, 9]. Since most of the water in the world is seawater, the desalination of seawater and brackish water is progressively gained attention.

In general, the term of desalination is applied for the process of removing salts from water to produce fresh water. Fresh water is defined as that type of water containing less than 1000 mg L^{-1} of salts or total dissolved solids (TDS). The desalination processes are commonly categorized into three categories regarding the associated separation mechanism: thermal phase change, interaction with selective membranes and electrostatic interaction. Multi-effect distillation (MEF), multi-stage flash distillation (MSF), vapor compression and freeze desalination (FD) are distinguished among the thermal phase change processes, while RO, FO and membrane distillation (MD) employ a selective membrane to perform the salt water desalination [4]. On the other hand, the electrostatic techniques such as electrodialysis (ED) and capacitive deionization (CDI) are usually used with waters containing TDS lower than 3000 mg L^{-1}.

The conventional desalination methods require large amounts of energy and have often associated an environmental pollution. In addition, the ability to exploit these processes is limited in many parts of the world and emerging processes, like FO, might help to solve this problem.

Osmosis consists in the spontaneous flow of a solvent, generally water, across a membrane permeable by the solvent, but not by the solutes. The osmosis phenomenon have been used in seawater desalination since it was discovered by Nollet in 1748 [10, 11]. In 1968, it was suggested to apply osmosis from brackish water to seawater in order to develop a mechanical pressure that could be used to drive the RO desalination of a second brackish water stream [12]. In 1975, Kravath and Davis proposed to use semipermeable membranes in conjunction with concentrated nutrient solutions as a passive method of purifying seawater that can be used in rafts [13]. Nowadays, the application of the osmosis phenomenon extends from water treatment and food processing to power generation and novel methods to control drug delivery (Figure 1) [2].

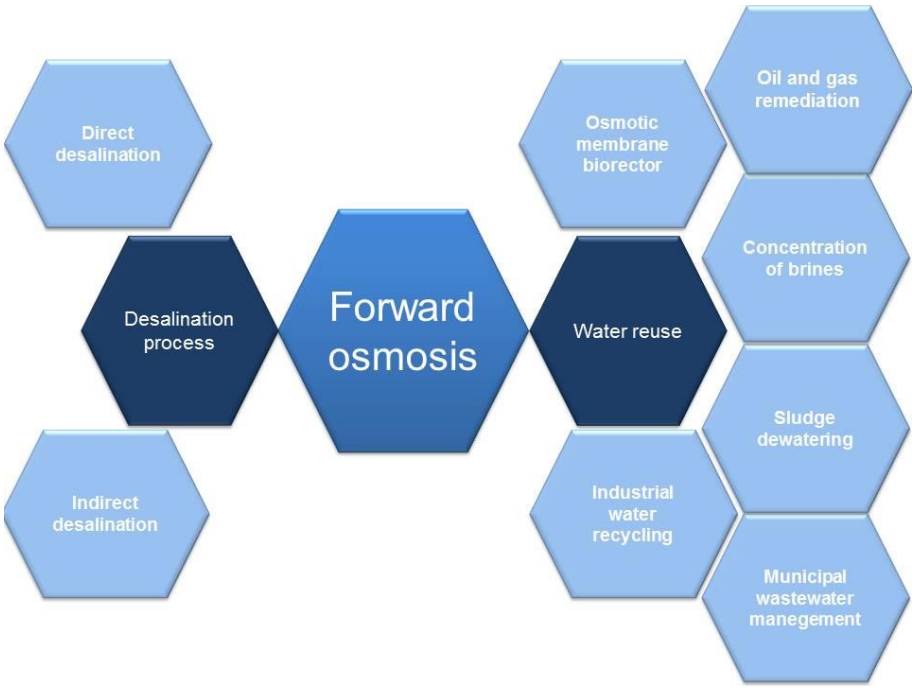

Figure 1: Applications of forward osmosis process in the water treatment industry. Figure adapted from [9].

FO is a membrane system that technically explores the natural phenomenon of osmosis, i.e., the pure water from a feed solution spontaneously flows through a semi-permeable membrane under an osmotic driving force provided by a more concentrated solution, known as draw solution (Figure 2) [14]. The type of feed solution can vary depending on the specific FO application; seawater, treated wastewater, brackish water, polluted water and even, distilled water can be employed [15].

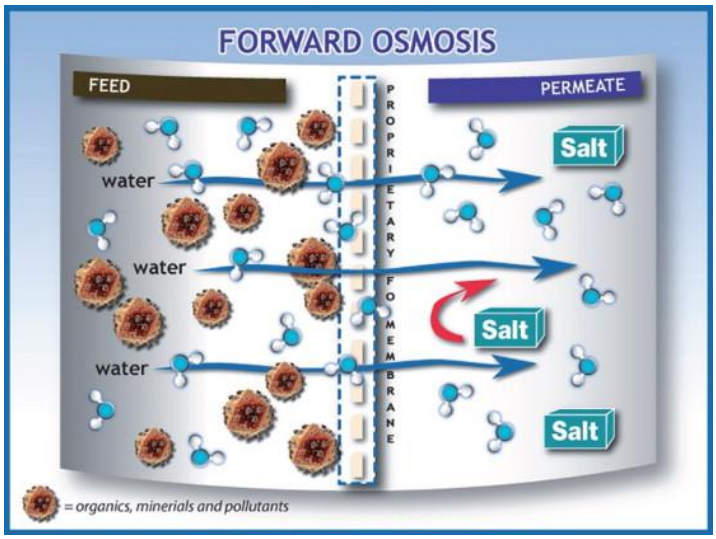

Figure 2: Scheme of the forward osmosis process. Figure reprinted from [16].

Some of the main advantages of FO include: the flexibility and applicability of the process due to the scalability of the membrane system; reduced membrane fouling propensity and simple cleaning compared to RO [17]; low electrical energy demand possible with a suitable

draw post-treatment step using low grade heat [2, 14]; rejection of particles, pathogens and harmful emerging substances, as well as TDS from complex solutions. Due to the lack of high hydraulic pressures, FO has also proven excellent conditions in terms of durability, reliability and water quality for highly polluted waters [17].

2.1.1 Osmotic pressure

Two solutions with different concentration create a gradient that drives water across the membrane from the low salt concentration side to that more concentrated. The water flow continues until the chemical potentials become equal on both sides of the membrane [18]. Therefore, the osmotic pressure (π) is equivalent to the pressure needed on the more concentrated solution to prevent the transport of water across the membrane. The osmotic pressure (π) can be defined by the van't Hoff equation (eq. 1) [19]:

$$\pi = \frac{iC_s RT}{M_w} \qquad \textbf{(eq. 1)}$$

where i is the van't Hoff factor, C_s is the solute concentration (g L^{-1}), R is the gas constant (L atm mol^{-1} K^{-1}), T is the temperature (K) and M_w is the molecular weight (g mol^{-1}).

The van't Hoff factor (i) is the ratio between the concentration of particles produced when the substance is dissolved, and the concentration of a substance as calculated from its mass. For most non-electrolytes dissolved in water is essentially 1. For most ionic compounds dissolved in water, the van't Hoff factor is equal to the number of discrete ions in a formula unit of the substance [20].

2.1.2 Factors influencing the FO process

The breakthrough and broad commercialization of the FO processes for desalination must be achieved through the research of new materials to be incorporated in membranes, the membrane fabrication and the design of efficient draw solutes [5]. Thus, the efficiency of the FO process can be modified and enhanced by factors related with the membrane characteristics, draw and feed solutions properties and the FO operating parameters [21]. These factors affecting on the flux performance are very significant, because they determine the productivity, and lately, the viability of the technology [14]. The main factors affecting on the FO performance are:

i. Temperature: like in other membrane processes, this factor plays a significant role in the performance of the FO process, since it has a direct influence on the thermodynamic

properties of the draw and the feed solutions and as consequence, the osmotic pressure increases with the temperature as observed in eq. 1 [22].

ii. Membrane module configuration: the packing of the membrane into the module must maximize the membranes surface in contact with the solutions as well as should reduce the deposition of particles resulting from the corresponding cross-flow [17]. Laboratory scale modules have been designed for flat sheet or tubular/capillary membranes, while modules for flat sheet membranes in plate-and-frame configuration are preferred at large scale [2]. Modules with spiral-wound and bag configurations can be also built, although they have received less attention. Since each mentioned configuration has advantages and drawbacks, there is no a perfect membrane module configuration.
An important parameter prior to the design the membrane module is the operation mode, i.e., continuous flow or batch operation. In continuous flow, the draw solution is repeatedly reconcentrated and reused and thus, modules implementing flat sheet membranes are more complicated to build and operate than in bath operation. In addition, the draw solution is diluted once in batch mode and not reconcentrated for further use [23].

iii. Membrane orientation: this factor is important because water flux behavior depends on the different membrane orientations, even with identical concentrations of draw solution [24].

iv. Draw solution (DS): an appropriate draw solution does not only promots the efficiency of the FO process, but also saves costs of the subsequent steps in recovering and replenishing the draw solute [25]. The main characteristics of an appropriate draw solution are:

- minimal toxicity, low cost, ideally inert, stable and with near neutral pH;
- high osmotic efficiency, i.e., high solubility in water and relatively low molecular weight;
- the reverse solute flux (J_s) of the draw solute must be minimal [20]. It arises by the high concentration difference between both draw the feed solutions, reducing the driving force and contaminating the feed solution, as well as also increasing the replenishment cost of the draw solute;
- easy regeneration of the diluted draw solution. FO is usually coupled with another process to produce clean water [20];
- compatibility with the membrane, i.e. it cannot be harmful for the membrane, chemically and physically [26, 27].

For seawater desalination, various types of draw solutions have been investigated, such as NaCl, NH_4HCO_3, urea, KCl, $CaCl_2$, $MgSO_4$ and Na_2SO_4 [20, 21].

v. Draw solution (DS) concentration: an increase of the DS concentration leads to a higher water flux, pumping energy required, feed recovery rates obtained, while decreasing the membrane area and operation time, as indicated in Figure 3 [21].

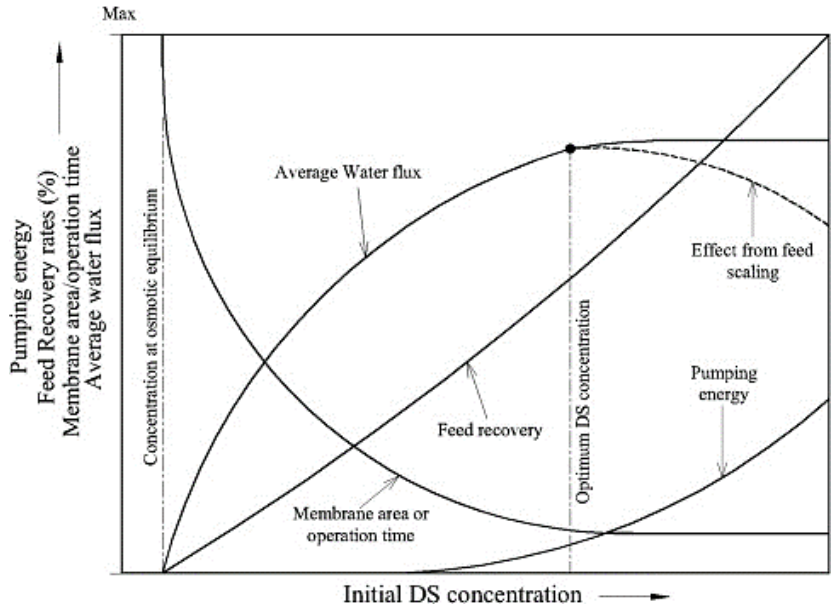

Figure 3: Correlation of the water flux, feed recovery rates, membrane area and pumping energy with the initial DS concentration used in FO. Figure reprinted from [21].

2.1.3 Limitations of the FO process

The major problem in FO is the decrease of the overall membrane permeability over time due to the concentration polarization (CP) and the membrane fouling, because both phenomena cause extra resistance of the membrane and consequently, slow down the water transport [23].

The low water flux is often attributed to problems of water transport phenomena across the membrane [2, 28-30]. However, the CP also has influence on this transport, CP depending on the correlation between flux, rejection and diffusion. FO membranes have generally an asymmetric structure with two different layers: an active layer (AL) and a support layer (SL). The AL is generally the dense selective layer and the porous SL provides the mechanical strength. Due to the asymmetry, the FO membranes can be positioned either with the AL faced to the feed solution (ALFS) or the draw solution (ALDS) during the FO experiments [31]. In the FO process, CP can take place on both sides of the membrane, although SL is generally the main reason of the bad performance of osmotically driven membrane processes [17]. On other hand, asymmetric membranes can present two types of CP phenomena: external and internal. Internal concentration polarization (ICP) generally occurs within the porous SL of the membrane, while external concentration polarization (ECP) takes place at the surface of AL.

Another limitation of the FO process is the fouling consisting in the accumulation of retained molecules or particles in the pores of the membrane or at the membrane surface [23]. Lower membrane fouling implies more transported water, less cleaning needed and longer membrane lifetime, as well as lower operational costs [6]. In general, the fouling observed in FO is related with the accelerated cake-enhanced osmotic pressure (CEOP) due to the reverse salt diffusion from the draw solution [32]. When the draw solution is facing the membrane support layer (ALFS, Figure 4a), the draw solute accumulates at the surface of the active layer through reverse diffusion, enhancing the concentration polarization layer and reducing the effective osmotic driving force. This phenomenon is less significant when the ALDS orientation is used (Figure 4b).

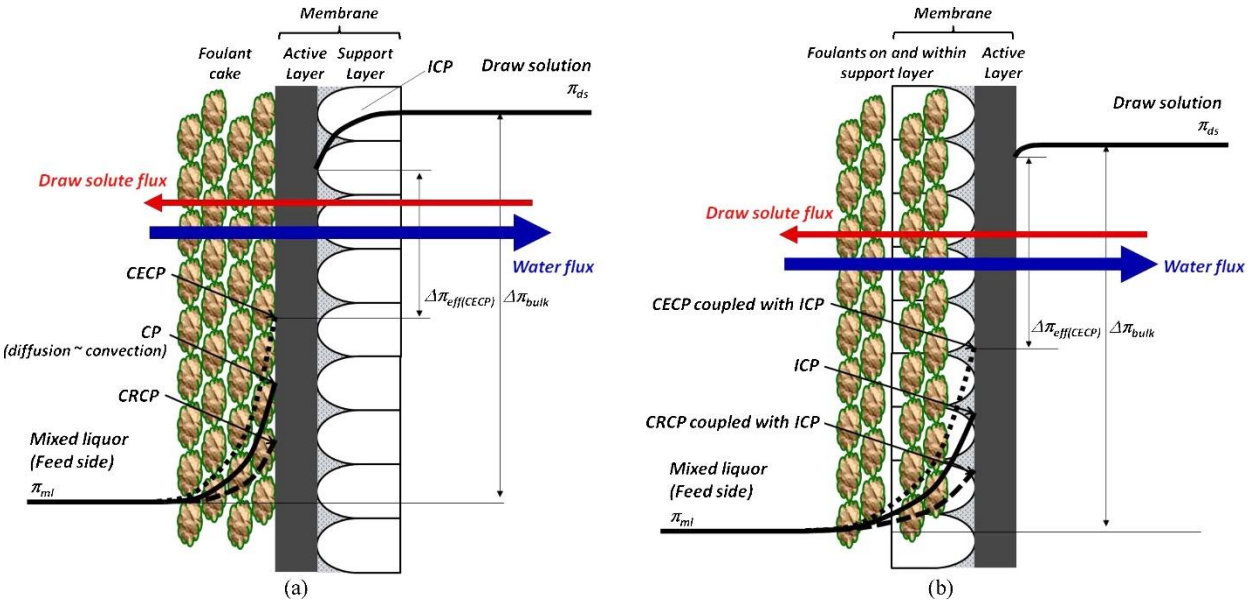

Figure 4: Fouling and concentration polarization effects for a FO system with membrane orientation of (a) ALFS and (b) ALDS. Figure reprinted from [14].

Currently, ICP is still a concern for FO and the main driver for further membrane development, since the membrane fouling in FO is completely reversible due to the lack of hydraulic pressure [33].

2.1.4 Membranes for FO

Asymmetric cellulose acetate (CA) membranes were the first employed for FO during the 1960's [34]. However, these membranes, which were specifically designed for RO, presented transport limitations due to their hydrophobicity and relatively thick support layer [35].

The breakthrough of the membranes applied for FO came with the development of thin and tailored cellulose triacetate (CTA) membranes (~50 mm) by Hydration Technology Innovations (HTI, Albany), which presented high water fluxes and reduced ICP [31]. Nowadays,

most of the commercially available membranes are made of CTA and polyamide thin-film composite (TFC), manufactured by HTI (Albany) and Oasys Water (Boston) [25].

On the other hand, FO membranes should allow fast transport of water towards the draw side, without migration of solutes between the draw and feed solutions. The loss of the osmotic agent to the environment have to be avoided: (i) to reduce the maintenance cost and the potential harmful environmental impacts; and (ii) to present modifications of the solubility characteristics and, lately, the need for periodic purge of the osmotic agent. Therefore, a FO membrane should have: (i) a dense, ultra-thin, active-separating layer for a high solute rejection; (ii) an open, thin, hydrophilic SL with high mechanical stability, sustaining long-term operation and reducing ICP; and (iii) a high affinity for water (hydrophilicity) for enhanced flux and reduced fouling propensity [23].

In Table 1 is shown an overview of some selected FO membranes, as well as specific experimental conditions in which they were tested.

Table 1: Brief overview of FO membranes summarizing some important experimental details and results.

Membrane	Draw solution	Feed solution	Orientation	J_w (L h^{-1} m^{-2})	J_s (g h^{-1} m^{-2})	Ref.
TS80 Nanofiltration (NF) TFC	1.5 M $MgSO_4$	DW	ALDS	1.1	n.d.	[36]
CA/CAT cast on a nylon fabric	1.2 M $MgSO_4$	0.6 M NaCl	ALDS	6.5	n.d.	[37]
Polybenzimidazole (PBI)-based dual layer NF	5.0 M $MgCl_2$	DW	ALFS	33.8	0.55	[38]
Dual-layer PBI-Polyethersulfone (PES)/Polyvinylpyrrolidone (PVP)	5.0 M $MgCl_2$	DW	ALDS	24.8	1.0	[38]
CA	2.0 M $MgCl_2$	DW	ALDS	7.3	0.53	[39]
Polyacrylonitrile (PAN) substrate, multiple polyallylamine hydrochloride and polystyrene sulfonate (PAH/PSS)	1.0 M $MgCl_2$	DW	ALFS	28	n.d.	[40]
CA-double dense layer	0.5 M $MgCl_2$	DW	ALDS	40-80	n.d.	[41]
Polyamide–imide (PAI) substrate treated by polyethyleneimine (PEI)	0.5 M $MgCl_2$	DW	ALFS	8.36 (1%PEI) 9.74 (2%PEI)	n.d.	[42]
PAI substrate treated by PEI	0.5 M $MgCl_2$	DW	ALDS ALFS	19.2 29.6	<0.5 <0.8	[43]
PES cast on polyethylene terephthalate (PET) fabric	3.0 M NaCl	DW	ALDS	32	8.76	[44]
PES/sulfonated polymer substrate	2.0 M NaCl	DW	ALFS	33	n.d.	[45]
CTA	1.0 M NaCl	DW	ALDS ALFS	15.8 26.8	12.18 19.07	[46]
TFC polyamide	0.5 M NaCl	DW	ALDS ALFS	32.2 14	3.54 10.6	[41]
Asymmetric CA	0.5 M NaCl	Fresh Water	ALDS	1.3	n.d.	[47]
CTA	6 M NH_4HCO_3	0.5 M NaCl	ALFS	23	n.d.	[31]

n.d.: not determined

2.2 Motivation and objectives of the thesis

In previous sections, the factors and limitations influencing the FO process have been commented. Figure 5 summarizes the relationships between ICP, the reverse solute, the membrane fouling, the membrane properties and the draw solute characteristics. The membrane fouling decreases with the reverse solute diffusion and ICP with draw solutes consisting of small ion sizes [33], although it also increases the reverse solute diffusion and, consequently, the membrane fouling. Thus, a compromise is necessary. Besides the draw solute properties, ICP, reverse solute diffusion and membrane fouling are also determined by the membrane characteristics [6]. Thereby, the performance of the FO process can be modulated by changing parameters intimately related with the process, such as temperature, membrane module configuration, type and concentration of draw solution and, on the other hand, developing new membranes, namely TFC membranes which can be easily prepared in the laboratory and are widely used in FO, as observed in Table 1.

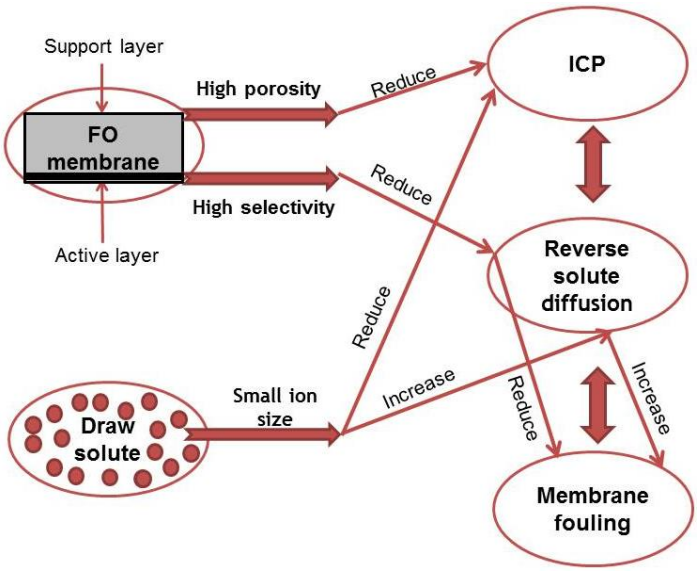

Figure 5: Correlations between the factors and limitations affecting the FO process. Figure adapted from [6].

In a previous MSc Thesis [18], different polysulfone (PS) membranes blended with carbon nanotubes (CNTs), graphene oxide (GO) and carbon-TiO_2 composites were prepared by the phase inversion method and used as support of TFC membranes, which were tested in a FO prototype with DI water and 0.6 M NaCl as feed and draw solutions. The home-made TFC membranes were active in the process, the membrane prepared with 0.6 wt.% of GO-TiO_2 composite presenting a water flux of 12.1 L h^{-1} m^{-2} and a salt rejection of 99 % [18].

In the present Thesis, the following specific scientific objectives were identified:

- To prepare TFC membranes on different hydrophilic commercial membranes, namely polyamide (PA), polyethersulfone (PES), mixed cellulose ester (MCE) and cellulose acetate (CA).

- To analyze the morphology, textural and chemical properties of TFC membranes.
- To study the performance of membranes in the filtration of DI water.
- To evaluate the performance of the TFC membranes in FO, namely water flux and salt rejection, at the same time studying and optimizing the following operating parameters: solution flow rates, membrane module configuration, membrane orientation and type and concentration of the draw solution.
- To assess the best TFC membrane in the FO system optimized by using seawater as feed solution.

Finally, the main technological objective of this Thesis was to design a TFC membrane with high water flux and excellent salt rejection to be used in seawater desalination driven by an optimized FO system.

3 Experimental

3.1 Materials

Sodium chloride (NaCl, 99.5 %), n-hexane (C_6H_6, >99 %), magnesium chlroride ($MgCl_2 \cdot 6H_2O$, 99 %) and potasium chloride (KCl, 99.5 %) were supplied from Merck, while magnesium sulfate ($MgSO_4$, 96 %) and nitric acid (HNO_3, 65 wt.%) were obtained from Panreac and Fluka, respectively. 1,3-phenylendiamine (MPD, 99 %) and 1,3,5-benzenetricarbonyl trichloride (TMC, 98 %) were purchased from Sigma-Aldrich.

Pure polyamide (PA), polyethersulfone (PES) and cellulose acetate (CA) membranes with 0.22 μm pore size and 25 mm of diameter were purchased from GE Healthcare, Millipore and Filtres Fioroni, respectively, while mixed cellulose ester (MCE) membranes with 0.45 μm pore size and 25 mm of diameter were supplied from Whatman™.

3.2 Thin-film composite (TFC) membranes

All the commercial membranes referred above were employed as support to prepare TFC membranes. The active polyamide layer was formed by interfacial polymerization (IP) on the surface of the membrane following a methodology adapted from [18, 48]. In a typical run, the commercial membrane was heated at 343 K in a deionized (DI) water bath for 2 min and the IP process was immediately carried out before it was cooled down to room temperature. For this purpose, an aqueous MPD solution (2 % w/v) was poured onto the membrane surface for 2 min, ensuring the penetration of the MPD solution into the membrane pores. The excess of the MPD solution was removed with a rubber roller. Then, a TMC solution (0.1% w/v) was poured onto the membrane surface for 1 min, the IP process taken place onto the surface. After that, the TFC membrane was immersed in pure n-hexane for 1 min in order to remove unreacted monomers from the TFC membrane surface. Finally, the TFC membranes were stored in DI water before used. TFC membranes are labelled by adding "TFC" to the corresponding commercial name of the membrane support. For instance, PES-TFC corresponds to the TFC membrane prepared on a commercial PES membrane.

3.3 Characterization of the membranes

Membranes morphology was investigated by scanning electron microscopy (SEM) using a FEI Quanta 400FEG ESEM/EDAX Genesis X4M instrument (accelerating voltage of 15 kV and a

working distance of ca. 10-15 mm). The membranes were frozen by using nitrogen. The microscope was equipped with a special multiple sample holder, in which the broken membranes were vertically positioned to analyze the cross-section of the membranes.

Thermogravimetric (TG) and differential thermogravimetric (DTG) analyses of the membranes were performed using a STA 490 PC/4/H Luxx Netzsch thermal analyser, by heating the sample in helium flow from 50 to 900 ºC at 20 ºC min^{-1}.

The hydrophilicity of the membrane surface was determined by water contact angle measurements using Attension (model Theta) equipment that allowed image acquisition and data analysis. The measurements were performed at room temperature, using the sessile drop method of water on dry membranes. Each contact angle was measured for at least 5 different locations on the membranes to determine the average value.

The overall porosity (ε) of the membranes was determined by the gravimetric method (eq. 2), following a procedure similar to that reported elsewhere [49]. After measuring the dry weight of the membranes, they were immersed into isopropyl alcohol (IPA) overnight to assure the solvent penetration into the membrane pores and then their wet weight was registered.

$$\varepsilon\ (\%) = \frac{(m_w - m_d)/\rho_{IPA}}{(m_w - m_d)/\rho_{IPA} + m_d/\rho_p} \times 100 \qquad \textbf{(eq. 2)}$$

where m_w and m_d are the weights of the wet and dry membranes, respectively, and ρ_{IPA} and ρ_p are the IPA (0.786 g cm^{-3}) and polymer (1.37, 1.15, 1.52 and 1.28 g cm^{-3} for PES, PA, MCE and CA, respectively) densities, respectively. Four membranes prepared by the same methodology were used to determine an average value of the porosity for each type of membrane, the standard deviation found being lower than ± 1 %.

N_2 adsorption-desorption isotherms at -196 ºC were obtained using a Quantachrome NOVA 4200e multi-station apparatus. The apparent surface area (S_{BET}) was determined by applying the Brunauer–Emmett-Teller (BET) equation [50]. The volume of N_2 adsorbed at a relative pressure of 0.95 (V_{pore}) was also calculated from the adsorption isotherms, which corresponds to the sum of the micro- and mesopore volumes according to Gurvitch's rule [51, 52].

The membrane thickness was measured using the Absolute Digimatic Indicator (ID-F543, Mitutoyo Co., Japan). The membrane was placed on the top of a highly softened granite surface and the height differences between the granite and membrane surfaces determine the membrane thickness. An average value was determined for each membrane by measuring different points of its surface.

3.4 Filtration

The performance of all membranes (i.e., with and without TFC layer) was evaluated through the determination of the permeate flux of DI water. Water flux measurements of the membranes were carried out in a stirred filtration cell (Millipore, model 8010). This cell has a total volume of 10 mL, an effective surface area of 4.1 cm^2 and operates at variable pressures and dead-end flows (Figure 6).

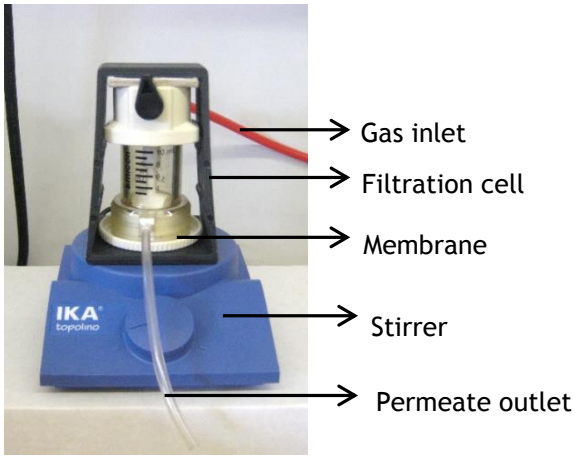

Figure 6: Stirred cell used for the water flux measurements

All membranes were initially soaked in an aqueous ethanol solution (30:70 v/v) for at least 2 h and then mounted on the filtration unit, which was filled with 10 mL of DI water. After that, the cell was pressurized and then the permeated volume at a given time was registered under steady flow and 298 K. The water flux (J_w, L h^{-1} m^{-2}) for each membrane was determined by applying eq. 3 and studied under variable trans-membrane pressures (TMP), ranging from 0.5 to 4.5 bar.

$$J_w = \frac{\Delta V}{A_m \times \Delta t} \qquad \textbf{(eq. 3)}$$

where ΔV is the permeate volume (L), A_m is the effective area of the membranes (m^2), and Δt is the sample time (h).

3.5 Forward osmosis

The performance of the TFC membranes was evaluated in a home-made FO unit (Figure 7), following a procedure reported elsewhere [18]. This FO unit basically consists of feed and draw reservoirs placed on weighting scales, a glass FO module and a peristaltic pump. The effect of operating variables such as membrane module configuration, membrane orientation, feed and draw flow rates and type and concentration of the draw solution on the membranes performance was studied.

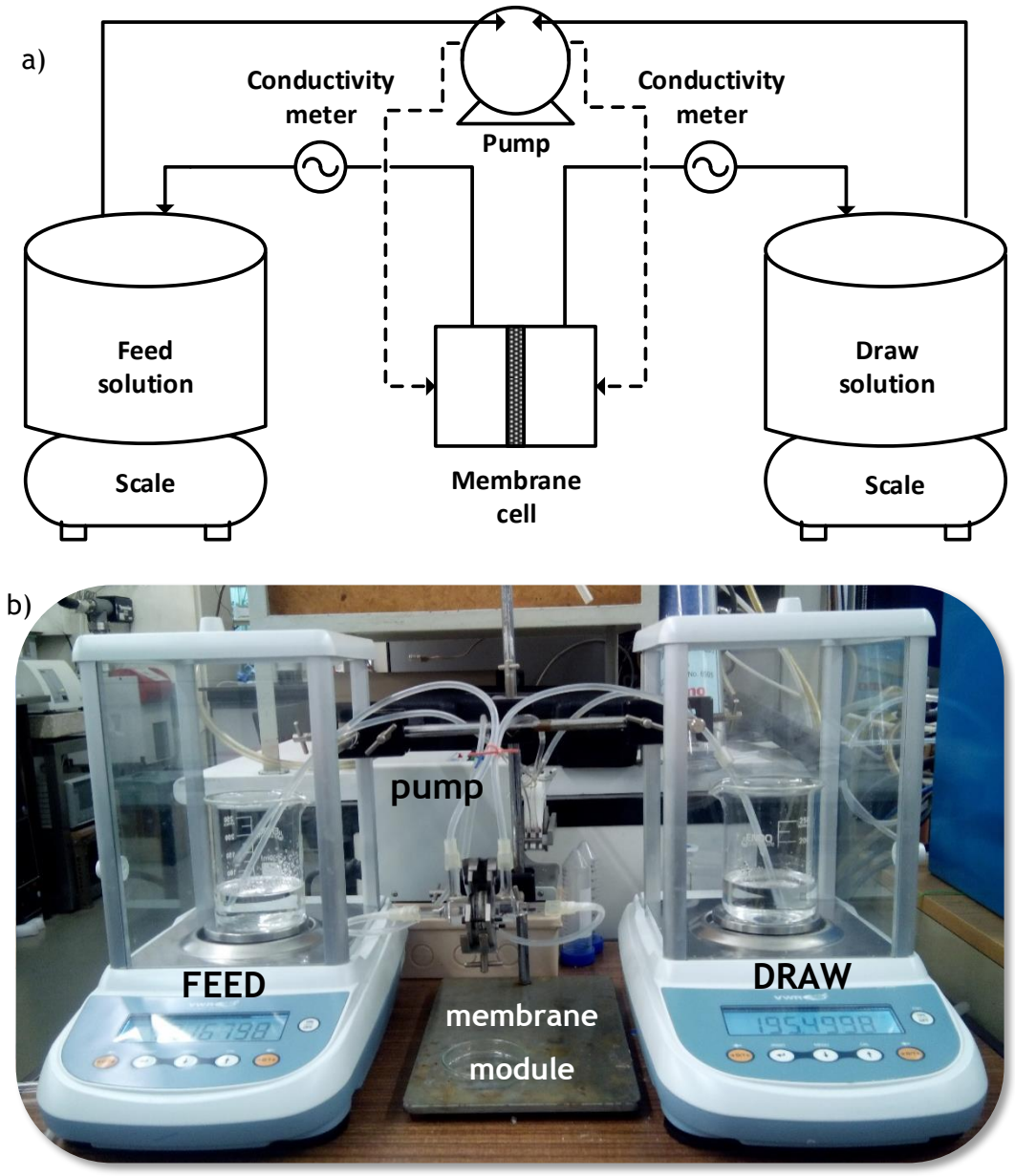

Figure 7: (a) Scheme and (b) image of the unit used in the FO experiments.

In a typical run, the membrane was placed into one of the glass modules operating in concurrent-flow (effective membrane area of 2 cm^2) and room temperature. Three different module configurations were specifically designed, one labelled as "W-cell", other as "H-cell" and another as "SS-cell", as shown in Figure 8. Then, 100 mL of DI (0.06 mM DI water - feed) and salty (0.6 M NaCl - draw) waters were pumped in recirculation mode at the same flow rate (Q_{feed} = Q_{draw} = 4, 9, 17 or 27 mL min^{-1}). The resulting osmotic pressure ($\Delta\pi$) difference between the feed and draw solutions was around 29 atm (determined from the van't Hoff equation eq. 1) for all the solutions with exception of $MgCl_2$ (44 atm). The water flux (J_w, eq. 3) was calculated by measuring the weight change of the feed and draw containers. Ionic conductivity was measured in both feed and draw streams by using online conductivity meters (VWR mod. 310) and by ion chromatography (Metrohm, mod. 881 Compact IC pro) to determine the

percentage of salt rejection (eq. 4). The concentration of specific cations and anions in the withdrawal samples were also analyzed with an ion chromatograph equipped with a cation and anion exchange column (Metrosep C4-250 and Metrosep A Supp 7-250, respectively).

$$\text{Ion rejection } (\%) = \left(1 - \frac{C_f}{C_d}\right) \times 100 \qquad \text{(eq. 4)}$$

where C_d and C_f are the concentrations of the draw and feed solutions, respectively.

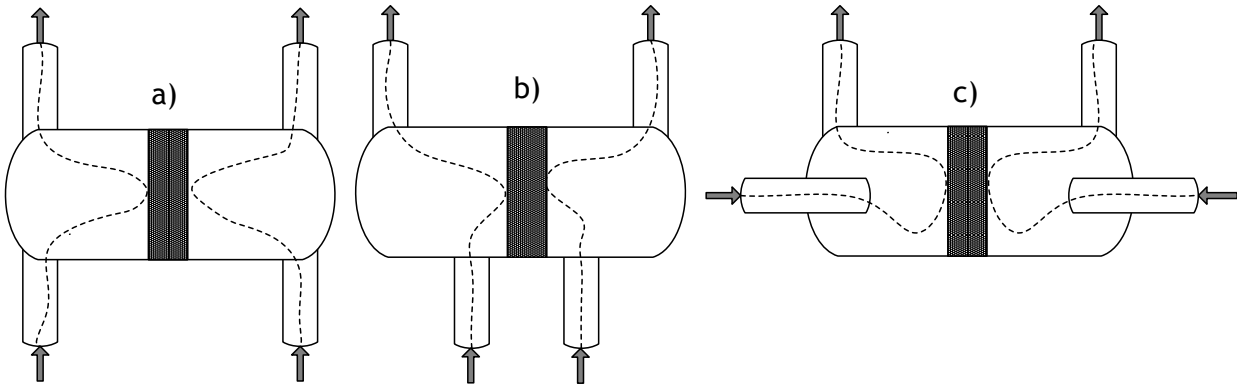

Figure 8: Schematic representation of the membrane module configurations: a) H-Cell; b) SS-Cell; c) W-Cell.

In FO experiments, the reverse solute flux (J_s, g h^{-1} m^{-2}) is another important parameter defining the membrane performance which indicates the amount of draw solute crossing the membrane from the draw side to the feed side, and it was determined from the increase of the feed conductivity by using eq. 5 [53]:

$$J_S = \frac{\Delta(C_t \times V_t)}{A \times \Delta T} \qquad \textbf{(eq. 5)}$$

where C_t is the salt concentration (determined with the conductivity meter) and V_t is the volume in the feed stream at given time (t).

The TFC membrane showing the best performance (PA-TFC) was tested by using DI water as feed solution and different draw solutions: (i) 0.6 M magnesium sulfate ($MgSO_4$) solution, (ii) 0.6 M magnesium chloride ($MgCl_2$) solution, and (iii) 0.6 M potassium chloride (KCl) solution. Further experiments were performed with the best draw solution (NaCl) and by varying its concentration to 2.0 M and 5.0 M, the osmotic pressure difference ($\Delta\pi$) being ca. 98 and 244 atm for these experiments, respectively.

At the final stage of this Thesis, and with the aim to verify the feasibility of the FO process for water desalination, a last experiment was carried out with a real sample as feed solution under the best operating conditions and membrane selected with DI water. The seawater sample was collected in the costal area of Leça da Palmeira (Portugal), with the following coordinates 41°11'57.7" N, 8°42'43.2" W.

4 Results and discussion

4.1 Characterization of the structured membranes

The morphology of the commercial and lab-prepared TFC membranes was analyzed by SEM. Figures 9 and 10 show representative SEM images of the cross-sections and top surfaces, respectively. The CA, MCE and PA membranes presented a symmetric structure (Figures 9a, c and g), while an asymmetric structure with a top dense layer and another porous sub-layer was only observed for PES (Figure 9e) and due to this fact, the micrograph magnification shown is different for this particular case. All commercial membranes presented the typical structure resulting from the crosslinking of the polymer chains during their corresponding preparation step. In the case of TFC membranes (Figures 9b, d, f and h), and as expected, differences with respect to the commercial membranes used as supports (Figures 9a, c, e and g), were only observed in the top surface. Thus, a polyamide thin layer was homogenously formed throughout the membrane surface with a thickness of ca. 20-30 nm.

The topography of the membranes was also very different when comparing PES (Figure 10e) and the other commercial membranes, i.e., CA, MCE and PA (Figures 10a, c and g, respectively). In fact, the PES membrane showed a heterogeneous pore size distribution, while the other membranes presented pores with similar sizes. On the other hand, the polyamide layer created on TFC membranes, partially coated the opened pore structure of the commercial membranes (Figures 10a-h).

All membranes did not present a significant development of the microporosity and mesoporosity, which is the typical range of porosity determined by physical adsorption of N_2 at 77 K. In this way, the values of S_{BET} and V_p collected in Table 2 were low and comparable for commercial membranes (e.g., S_{BET} varying from 11 to 26 $m^2\ g^{-1}$). Regarding the TFC membranes, only a certain porosity was detected for PES-TFC (in terms of V_p, i.e., 0.07 $cm^3\ g^{-1}$), since the other TFC membranes presented very low or negligible values of both S_{BET} and V_p.

In Table 2, the overall porosity obtained by applying the gravimetric method is also shown. The commercial membranes presented porosities ranging from 80 % to 85 %, while only slightly lower values were obtained for TFC membranes, i.e., 76-83 %. Regarding the mean pore size, only MCE has a pore size of 0.45 µm, while CA, PA and PES present a d_{pore} = 0.20, 0.20 and 0.22 µm, respectively.

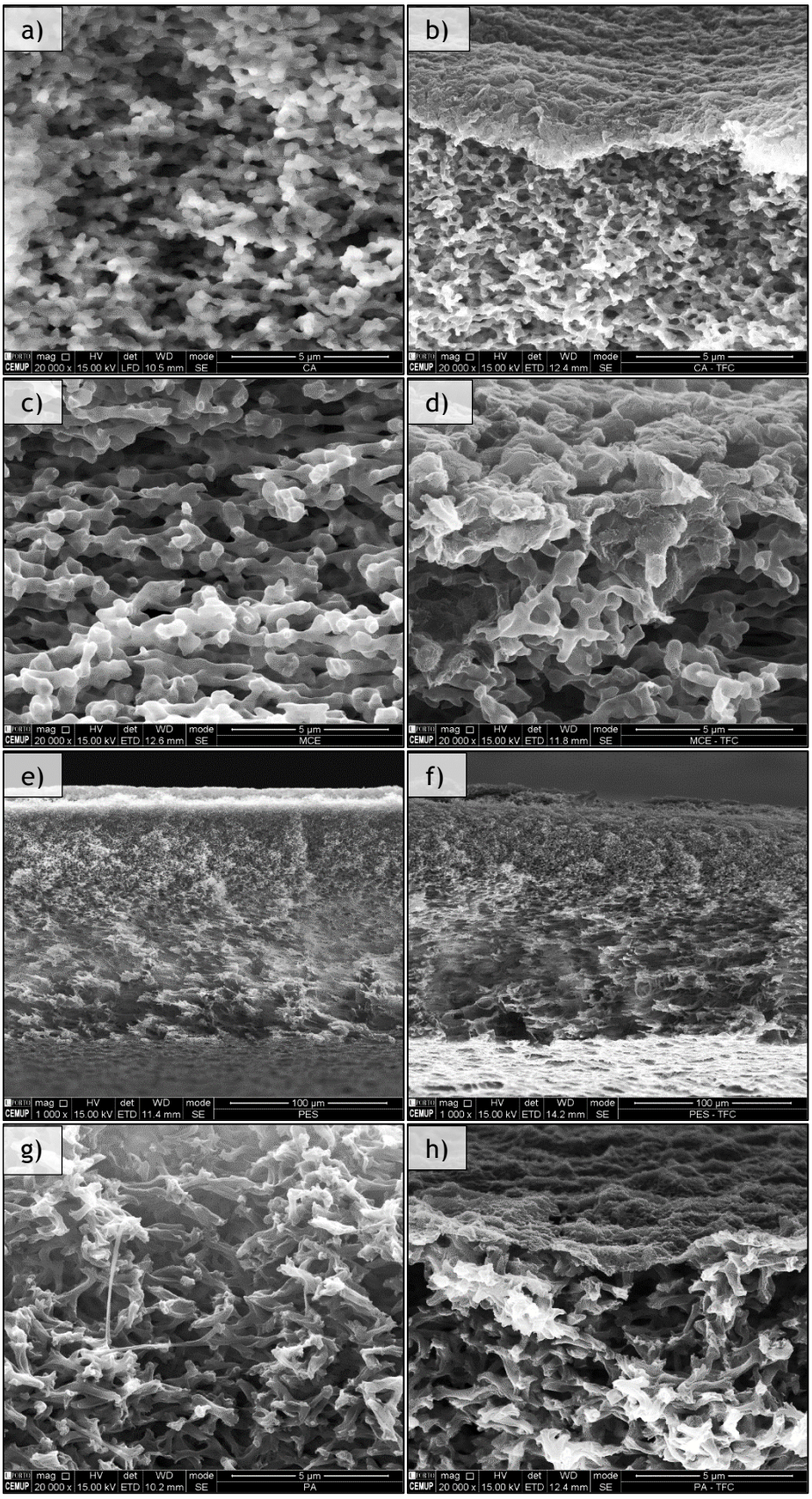

Figure 9: SEM micrographs of the cross section for the commercial and TFC membranes: (a) CA, (b) CA-TFC, (c) MCE, (d) MCE-TFC, (e) PES, (f) PES-TFC, (g) PA and (h) PA-TFC.

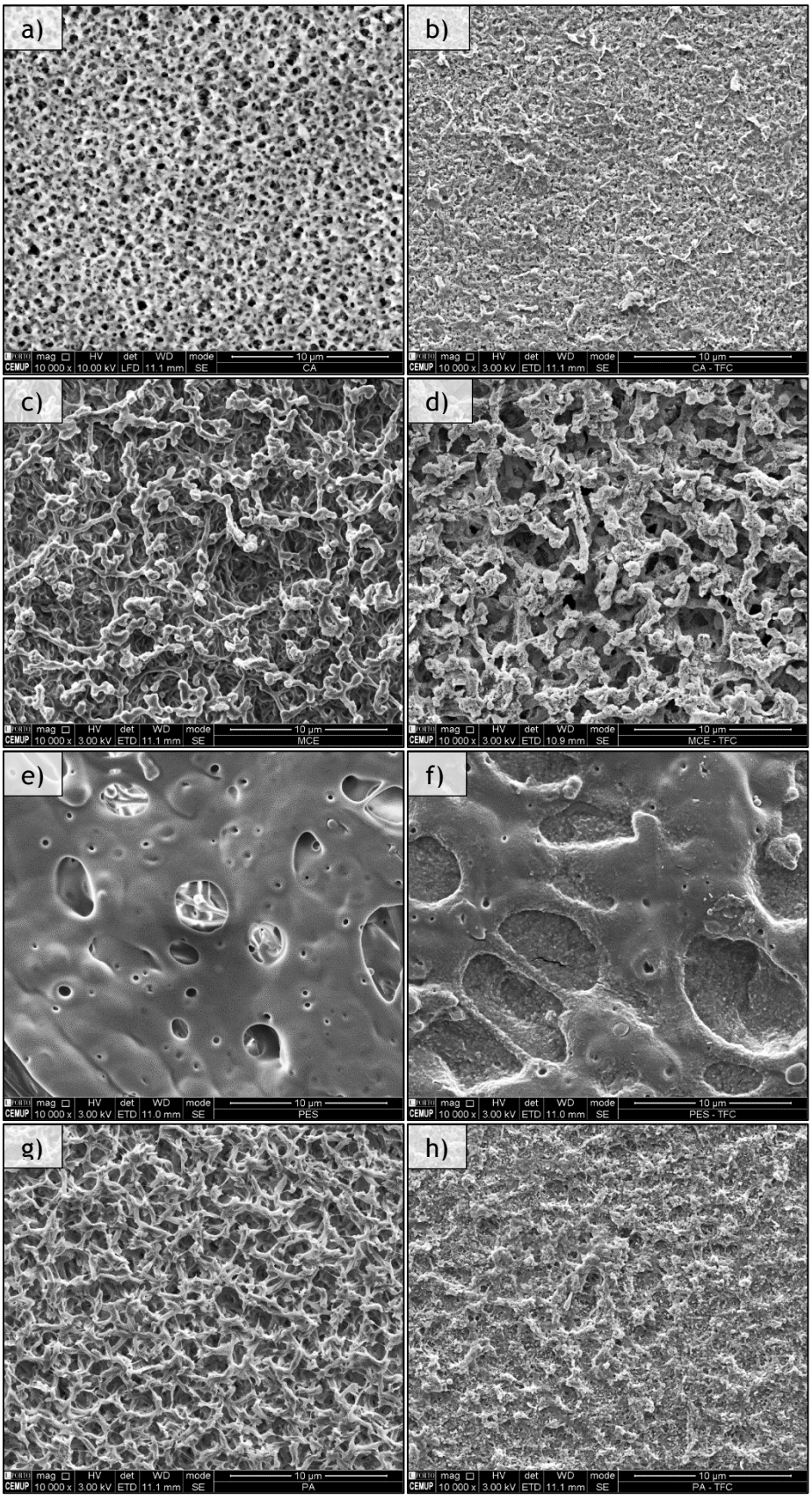

Figure 10: : SEM micrographs of the top surface for the commercial and TFC membranes: (a) CA, (b) CA-TFC, (c) MCE, (d) MCE-TFC, (e) PES, (f) PES-TFC, (g) PA and (h) PA-TFC.

The more notorious changes were observed in the surface hydrophilicity of the membranes (Table 2). MCE was the less hydrophilic membrane since presented the highest contact angle (93 °) compared to CA, PES and PA (59 °, 62 ° and 60 °, respectively). In the case of TFC membranes, PES-TFC was the most hydrophilic membrane (72 °), while CA-TFC, MCE-TFC and PA-TFC presented a contact angle around 79 °. In general, the TFC layer increases the contact angle of CA, PES and PA, while decreases that of MCE which is a hydrophobic support. Therefore the polyamide layer produces a decrease of the porosity, while the hydrophilicity could be influenced by the membrane roughness.

Table 2: Textural characterization, contact angle (°) and measurements of water flux for all membranes.

Membrane	Porosity (%)	S_{BET} ($m^2\ g^{-1}$)	V_{pore} ($cm^3\ g^{-1}$)	d_{pore} (μm)	Contact angle (°)	Thickness (mm)	J_w ($L\ h^{-1}\ m^{-2}$)
CA	83	15	0.04	0.20	59 ± 2	0.117	13365*
MCE	85	19	0.04	0.45	93 ± 2	0.140	15828*
PES	82	11	0.02	0.22	62 ± 2	0.170	12424*
PA	80	26	0.06	0.20	60 ± 2	0.134	6127*
CA-TFC	83	< 1	0.01	n.d.	78 ± 1	0.122	5.43†
MCE-TFC	79	< 1	0.01	n.d.	80 ± 2	0.140	7888†
PES-TFC	80	< 1	0.07	n.d.	72 ± 2	0.171	7.06†
PA-TFC	76	< 1	0.01	n.d.	78 ± 1	0.145	19.1†

n.d.= not determined; * determined at 0.5 bar TMP; † determined at 4.5 bar TMP.

The water flux (J_w) of all membranes was analyzed in the filtration of DI water (Table 2). The commercial membranes were analyzed at 0.5 bar TMP, while 4.5 bar TMP was selected for the TFC membranes. For commercial membranes, the flux varied in this order: MCE > CA > PES >> PA, which should be justified by the different porosity, pore diameter and hydrophilicity. In this context, MCE presented the highest pore diameter (0.45 μm) and, thereby, a larger amount of water is expected to across the membrane at a determined TMP. The results for CA, PES and PA are related with the porosity and contact angle of the membranes. In fact, the water flux measured varied in accordance with the membrane porosity.

Regarding TFC membranes, a worse permeation of water was observed compared to the commercial membranes (Table 2), since the water flux values were always lower (e.g., 13365 and 5.43 $L\ h^{-1}\ m^{-2}$ for PA and PA-TFC, respectively, even if a higher TMP was applied to PA-TFC). Therefore, the polyamide layer was successfully deposited on the commercial membrane to be

used in the FO experiments. For TFC membranes, the flux varied as follows: MCE-TFC >>> PA-TFC > PES-TFC > CA-TFC.

Figure 11 shows the TG/DTG curves obtained in inert atmosphere for the PA membrane with and without the polyamide layer (i.e., PA and PA-TFC). The main weight loss detected at 464 ºC and 454 ºC for PA and PA-TFC, respectively, was due to the decomposition of the polymer. Therefore, the polymerization interfacial method did not affect to the chemical properties of the original commercial membranes.

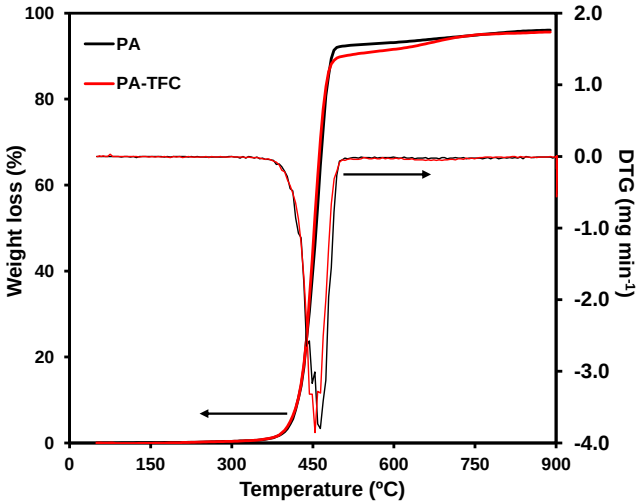

Figure 11: TG/DTG curves of the PA and PA-TFC membranes.

4.2 Forward osmosis

As previously mentioned, the driving force in FO is the osmotic pressure difference between the feed and draw solutions. The FO process can operate in two different modes by changing the orientation of the membrane active layer, i.e. active layer faced to the draw solution (ALDS) or active layer faced to the feed solution (ALFS) [54]. The performance of the TFC membranes in FO is mainly given by both water flux and ion rejection. Firstly, TFC membranes were tested in FO by using DI water and 0.6 M NaCl as feed and draw solutions, respectively. The TFC membrane with the best performance was then used to optimize the FO operating parameters to treat a real seawater sample.

4.2.1 Membranes screening

TFC membranes were firstly tested in ALDS configuration and the results are shown in Figures 12 and 13. In general, the water flux quickly increased during the first 20 min, and then remained relatively stable until 120 min (Figure 12). A non-linear increase in flux over time may be attributed to the presence of fouling or ICP [55].

The TFC membrane with the highest water flux was that prepared on a PA membrane regardless of the ALDS and ALFS orientation tested (10.7 and 10.2 L h^{-1} m^{-2}, respectively). The other TFC membranes (CA-TFC, MCE-TFC and PES-TFC) presented significantly lower water flux values compared to PA-TFC (e.g., 6.7 and 6.6 L h^{-1} m^{-2} for CA-TFC in ALDS and ALFS, respectively). MCE-TFC was expected to present (*a priori*) the highest water flux because this membranes showed a superior performance in filtration experiments (Table 2). However, the larger pore size can affect the hydraulic resistance of the FO process and, consequently, the water permeability [56].

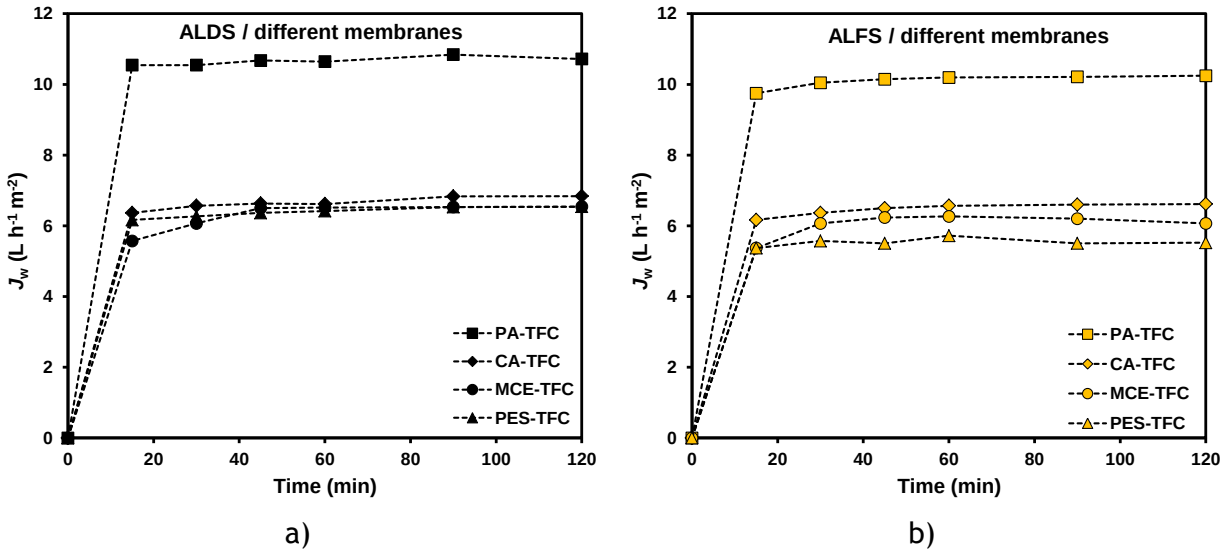

Figure 12: Water flux obtained in FO with W-cell for TFC membranes: (a) ALDS and (b) ALFS configurations (Q_{feed} = Q_{draw} = 17 mL min^{-1}).

In general, the results obtained in ALDS orientation are slightly better than those obtained in ALFS (Figures 12a and b, respectively). This fact is justified by the higher effective osmotic pressure difference and a lower contribution to the ICP effect in the ALDS orientation, since the dense active layer faces the concentrated draw solution [14]. Besides, the hydrophilic and highly porous substrate faces the feed solution in the ALDS orientation, and thus, water flows across the membrane with low resistance [53].

The best TFC membrane was also evaluated in terms of ion rejections (Cl^- and Na^+) and reverse solute flux (J_s) (Figure 13), which indicates the amount of draw solute (NaCl) passing through the membrane from the draw solution to the feed solution. In general, all membranes presented moderated reverse solute fluxes and the ion rejection was always above 99 % regardless the type of ion.

In agreement with the results described, PA-TFC was the most active membrane, i.e., highest water flux, moderate solute reverse flux and high ion rejection. Therefore, PA-TFC was selected to optimize the operating parameters in the FO process.

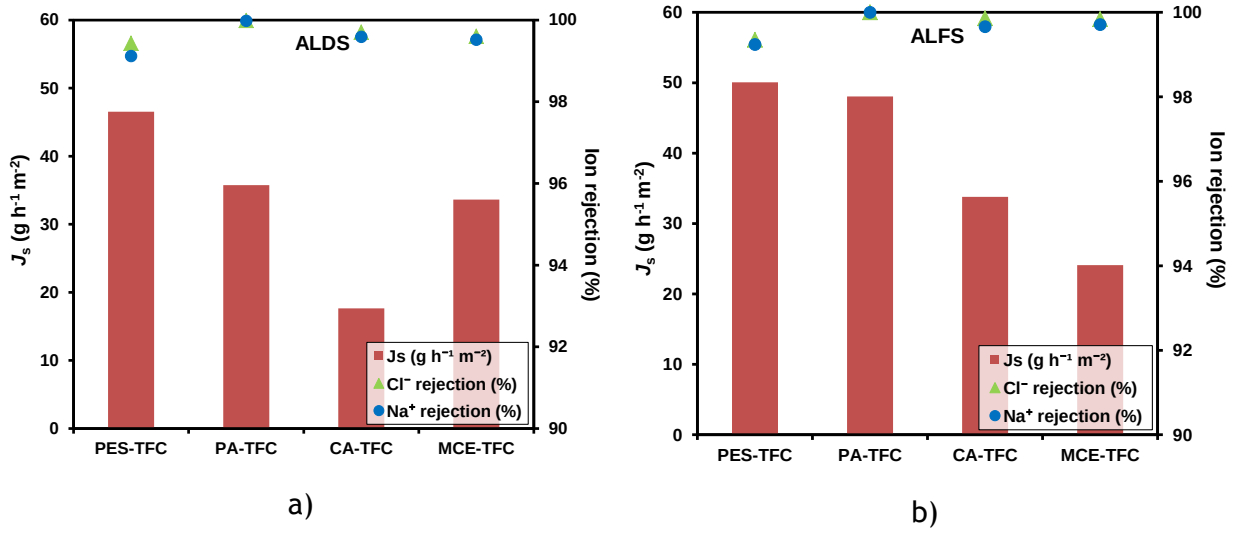

Figure 13: Reverse solute flux (J_s), Na^+ and Cl^- rejections (%) obtained in FO with W-cell for TFC membranes: (a) ALDS and (b) ALFS configurations (Q_{feed} = Q_{draw} = 17 mL min^{-1}).

4.2.2 Operating parameters: flow rate, membrane module configuration and type and concentration of draw solution

a) Different feed and draw flow rates (Q_{feed} = Q_{draw})

The first operating parameters to be optimized were the feed and the draw flow rates, which were studied at Q_{feed} = Q_{draw} = 4, 9, 17 and 27 mL min^{-1}, and membrane module configuration, i.e., H-cell, SS-cell and W-Cell. Figures 14 and 15 show the corresponding results obtained in FO for PA-TFC by using DI water and 0.6 M NaCl solution, as feed and draw solutions, respectively.

The permeance of PA-TFC increased with the flow rate from 4 mL min^{-1} up to an optimum value of 17 mL min^{-1}, regardless of the module configuration tested and orientation of the membrane (Figure 14). Increasing flow rates translate into increasing fluid velocity, which promotes a better mixing and a decrease of the CP effect, which influences on the effective pressure osmotic difference at both membrane sides. In addition, the lower CP between the membrane surface and the bulk phases may increase the mass transfer. In addition, the water flux obtained at 27 mL min^{-1} was not the highest probably due to the geometry and volume of the membrane modules designed, which did not favour the contact between the membrane surface and the liquid phase above 27 mL min^{-1}.

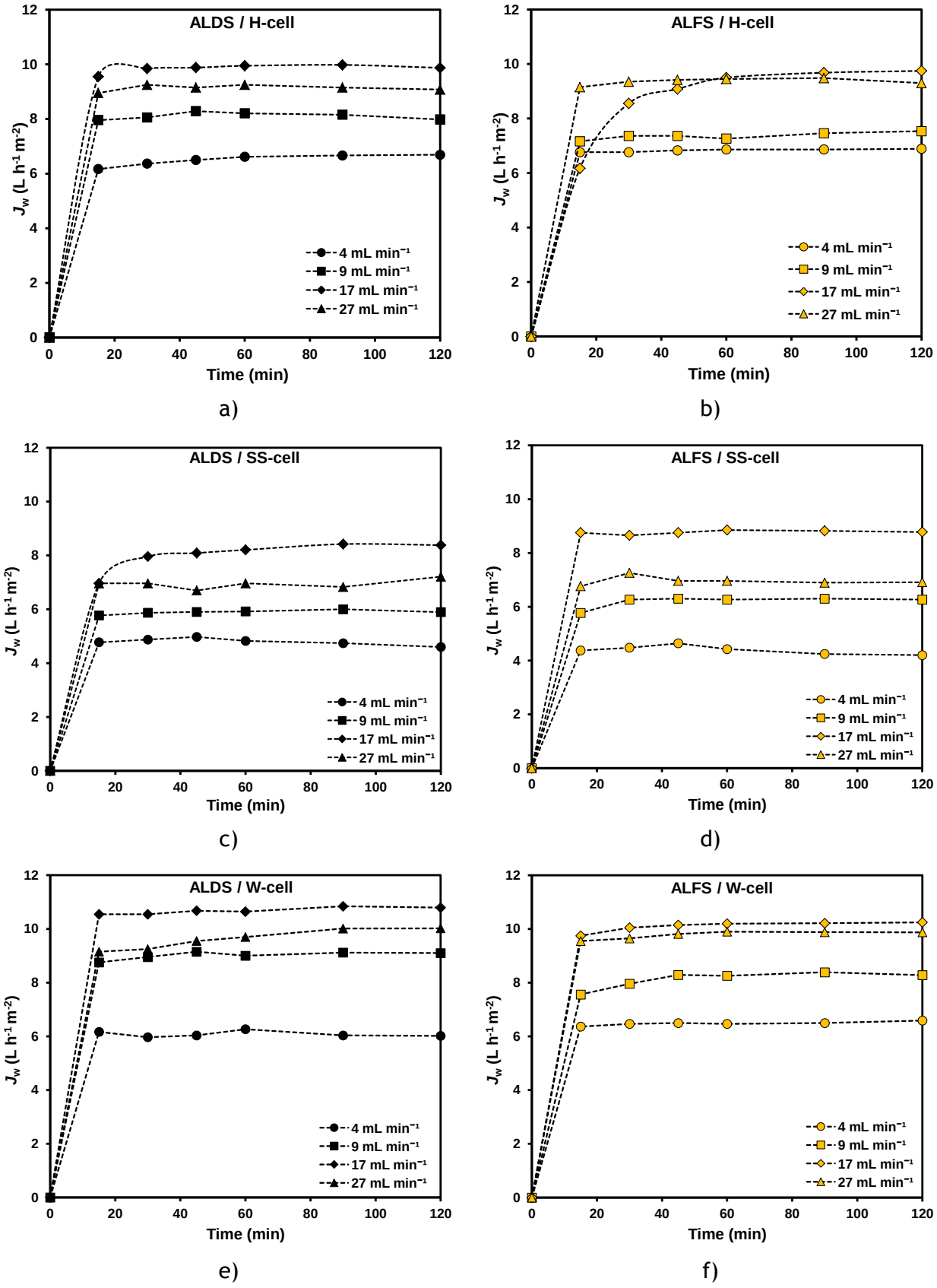

Figure 14: Water flux obtained in FO at different flow rates with different membrane module configurations for PA-TFC: (a, b) H-cell, (c, d) SS-cell and (e, f) W-cell; (a, c, e) ALDS and (b, d, f) ALFS configurations (DI water as feed solution).

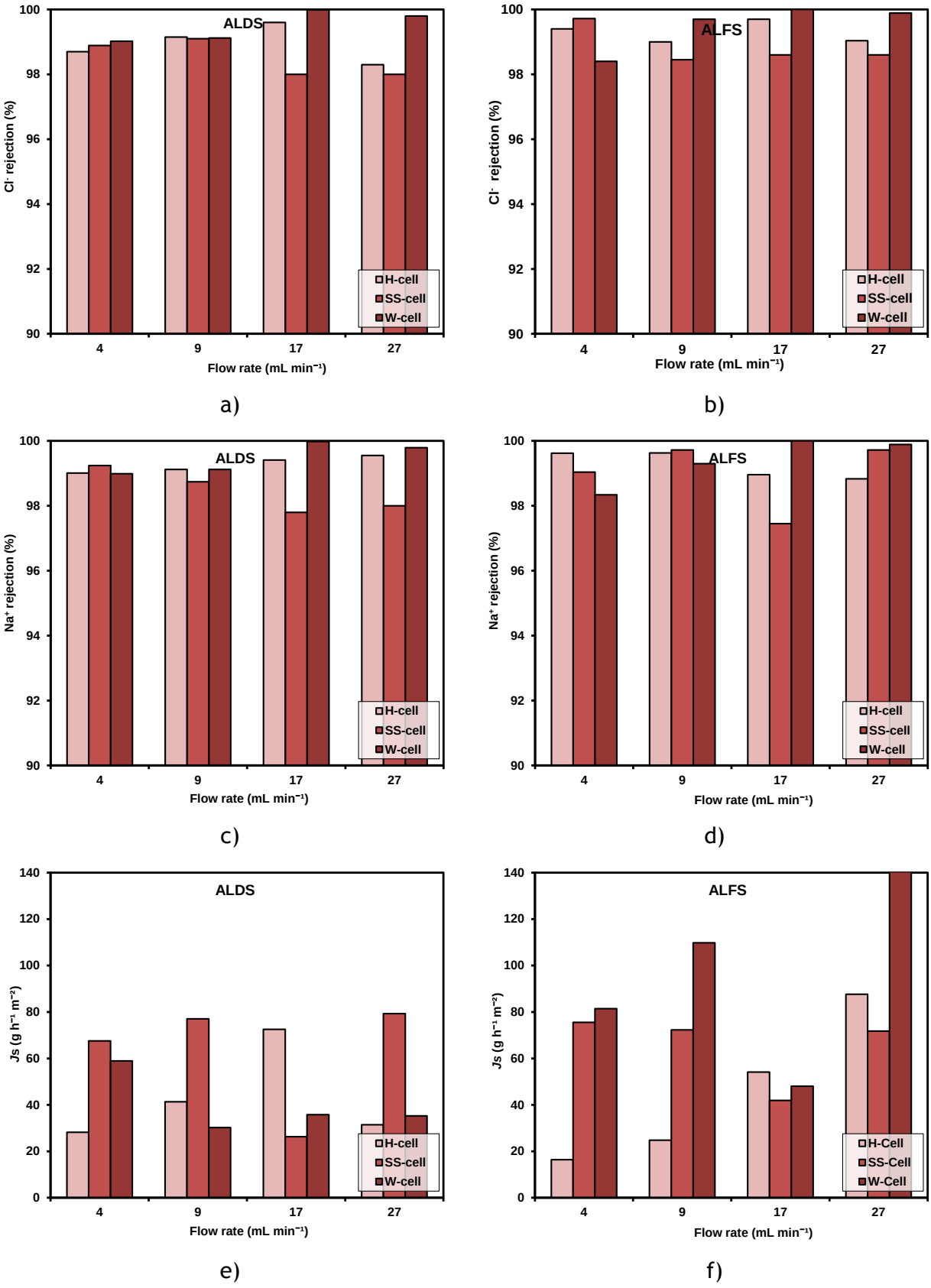

Figure 15: Reverse solute flux (e, f), Cl^- (a, b) and Na^+ (c, d) rejections obtained in FO at different flow rates with different membrane module configurations for PA-TFC: (a, c, e) ALDS and (b, d, f) ALFS configurations (DI water as feed solution).

On the other hand, the reverse solute flux should increase with the flux of the membrane in FO, as observed for H-cell (Figures 15a and b). However, a different behavior was observed depending on the membrane module employed. In general, a low J_s was determined at 17 mL min^{-1}, in particular for SS-cell and W-cell. In spite of the mentioned results, the ion rejections were always above 97 % regardless of the flow rate and the membrane module used (Figures 15a-d). Therefore, it is possible conclude that the optimal flow rate is 17 mL min^{-1}.

b) Different membrane module configurations

Although some results regarding the membrane modules were discussed above, Figure 16 summarizes the flux determined for each configuration at the optimum flow rate. The highest water flux in FO was obtained with the W-cell, then with H-cell and finally, SS-cell, regardless the membrane orientation used (J_w = 11.6, 10.7 and 8.3 L h^{-1} m^{-2}, respectively in ALDS). The different PA-TFC performance in the membrane modules could be related with the efficiency caused by decrease of mass transfer coefficient in the active layer.

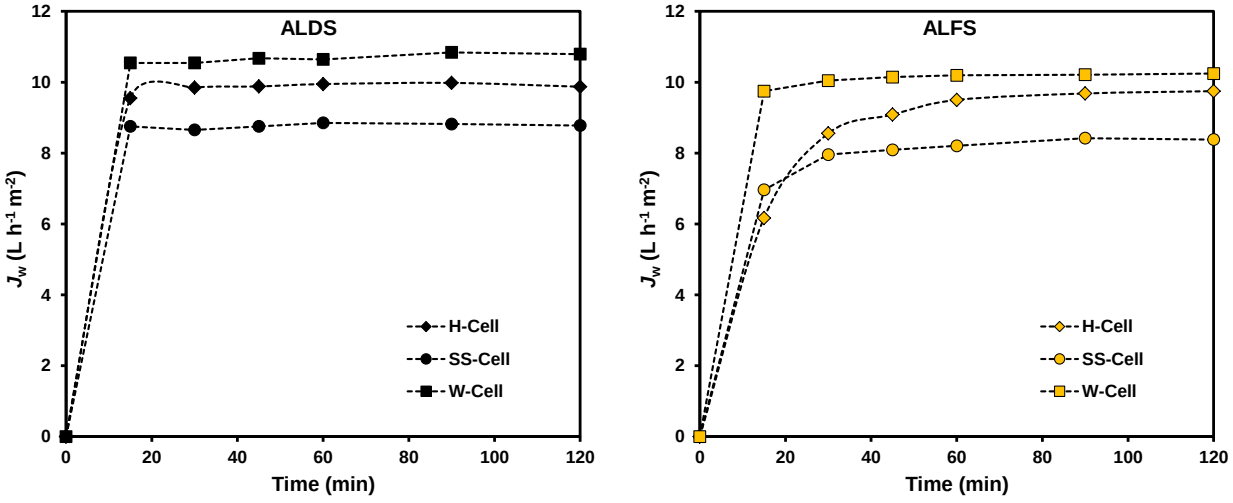

Figure 16: Water flux obtained in FO with different cells for PA-TFC: (a) ALDS and (b) ALFS configurations (DI water as feed solution; Q_{feed} = Q_{draw} = 17 mL min^{-1}).

Because PA-TFC presented good results in the W-cell in terms of water flux and reverse solute flux, this membrane configuration was selected for the next experiments.

c) Different draw solutions

Figures 17 and 18 show the results obtained in FO with different 0.6 M draw solutions, namely NaCl, $MgSO_4$, $MgCl_2$ and KCl. The flux determined with the different draw solutes varied in this order: NaCl > $MgCl_2$ > KCl > $MgSO_4$, regardless of the membrane orientation used (Figure 17). Therefore, PA-TFC obtained a better performance with NaCl as draw solute under the operating parameters already optimized.

Because the concentration for all draw solutions was fixed at 0.6 M, the resulting osmotic pressure difference at both membranes sides was around 29 atm for all solutions with exception of $MgCl_2$, which was 44 atm due to its different van't Hoff factor. Therefore, the different results obtained should be related with the different ion sizes of the draw solutes, their interaction with the membrane surface, their contribution to the ICP effect and the osmotic pressure difference. As previously described, ICP decreases with draw solutes composed by small ion sizes [33]. Therefore, a larger ICP effect is expected with $MgSO_4$ compared to $MgCl_2$, since the SO_4^{2-} size is bigger than that of Cl^-. In the same way, the Na^+ size is smaller than that for K^+ and, consequently, the induced ICP effect. However, this reasoning does not explain the worse results obtained with KCl compared to NaCl, the K^+ size being smaller than that of Na^+, as well as the better results obtained with NaCl, i.e., lower osmotic pressure than with MgCl.

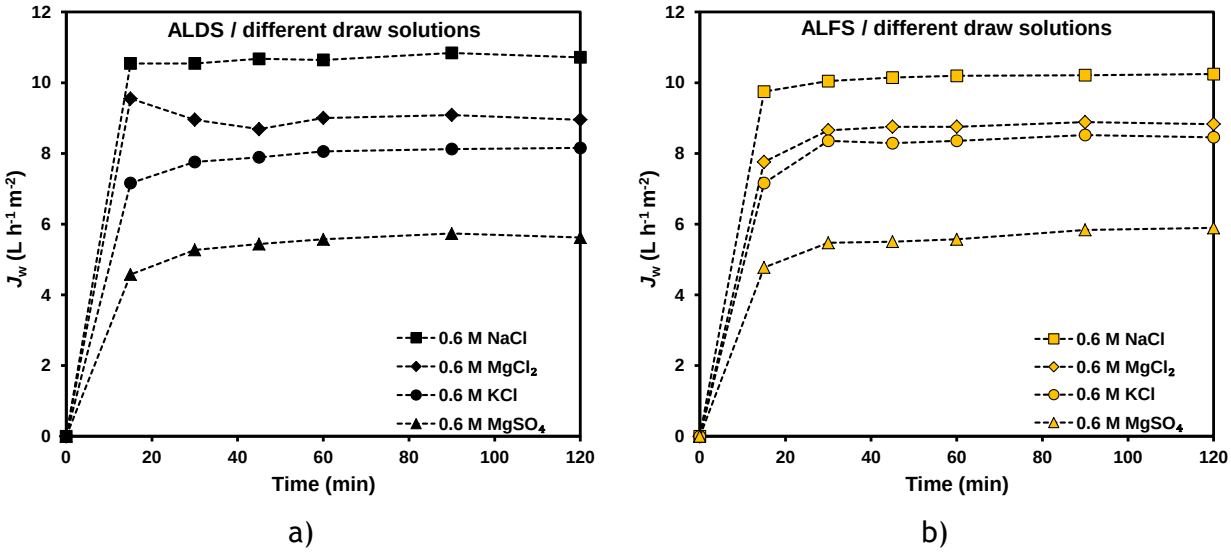

Figure 17: Water flux obtained in FO with different draw solutions for PA-TFC: (a) ALDS and (b) ALFS configurations (W-Cell; DI water as feed solution; Q_{feed} = Q_{draw} = 17 mL min^{-1}).

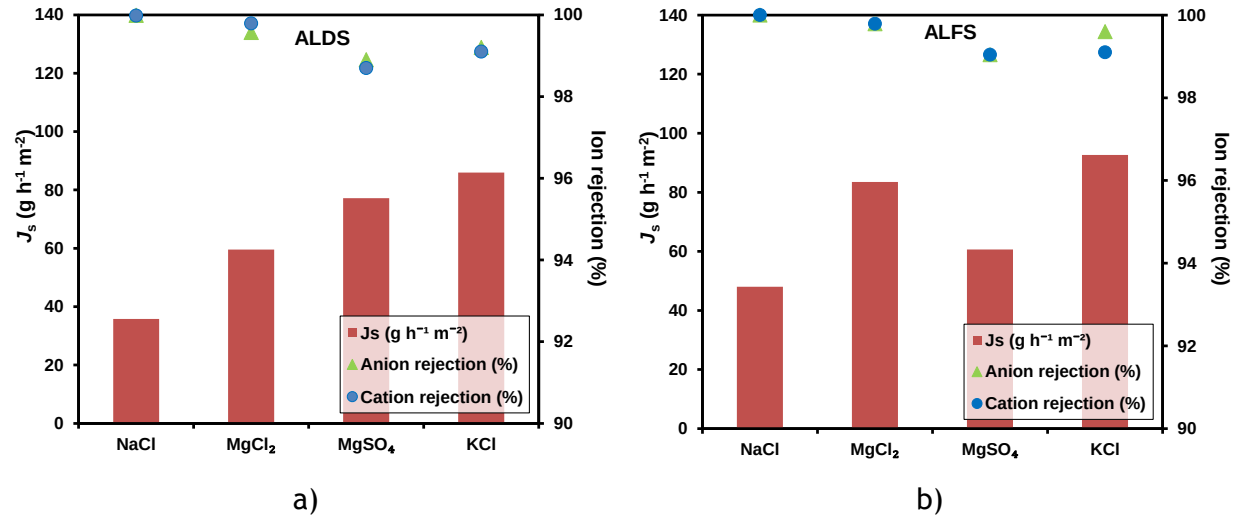

Figure 18: Reverse solute flux (J_s), cation and anion rejections (%) obtained in FO with different draw solutions for PA-TFC: (a) ALDS and (b) ALFS configurations (W-Cell; DI water as feed solution; Q_{feed} = Q_{draw} = 17 mL min^{-1}).

On the other hand, the ion sizes of the draw solute not only have influence on ICP but also on the membrane fouling. When the reverse solute flux is analyzed for each draw solution (Figure 18), a higher J_s is determined for both $MgCl_2$ and KCl compared to NaCl and, thus, a larger fouling is expected and a consequent lower water flux (Figure 17).

d) Different NaCl concentrations

Once NaCl was selected as better draw solute, different concentrations were studied, namely 2.0 M and 5.0 M. Figure 19 shows an increase of water flux with the NaCl concentration. This behavior is justified by the higher driving force related with higher NaCl concentrations [14, 21], since the osmotic pressure difference varied as follows: 29, 98 and 244, for 0.6 M, 2.0 M and 5.0 NaCl concentrations, respectively.

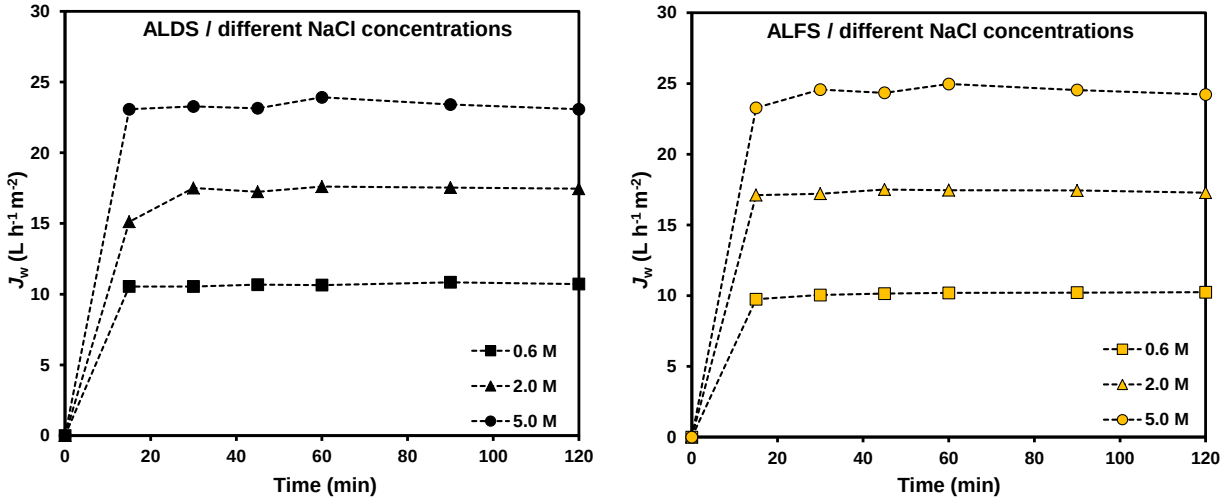

Figure 19: Water flux obtained in FO with different NaCl concentrations for PA-TFC: (a) ALDS and (b) ALFS configurations (W-Cell; DI water as feed solution; Q_{feed} = Q_{draw} = 17 mL min^{-1}).

The increase of the osmotic pressure difference obviously leads to a higher reverse solute flux (Figure 20) from 36 g h^{-1} m^{-2} to 124 g h^{-1} m^{-2} for 0.6 M and 5.0 M NaCl concentration, respectively in ALDS. These results indicate that the polyamide layer is better for rejection of ions until a certain concentration of draw solution (below 2.0 M NaCl). However, the values for ions rejection are always above 98 % and, thus, the significantly higher water flux obtained with 5.0 M NaCl in comparison with lower NaCl concentrations (Figure 19) justifies 5.0 M NaCl as the optimal draw concentration.

Therefore, it is possible to conclude that PA-TFC had the best performance in FO with the following parameters optimized: feed and draw flow rates of 17 mL min^{-1}, W-cell configuration, 5.0 M NaCl as draw solution and ALDS orientation.

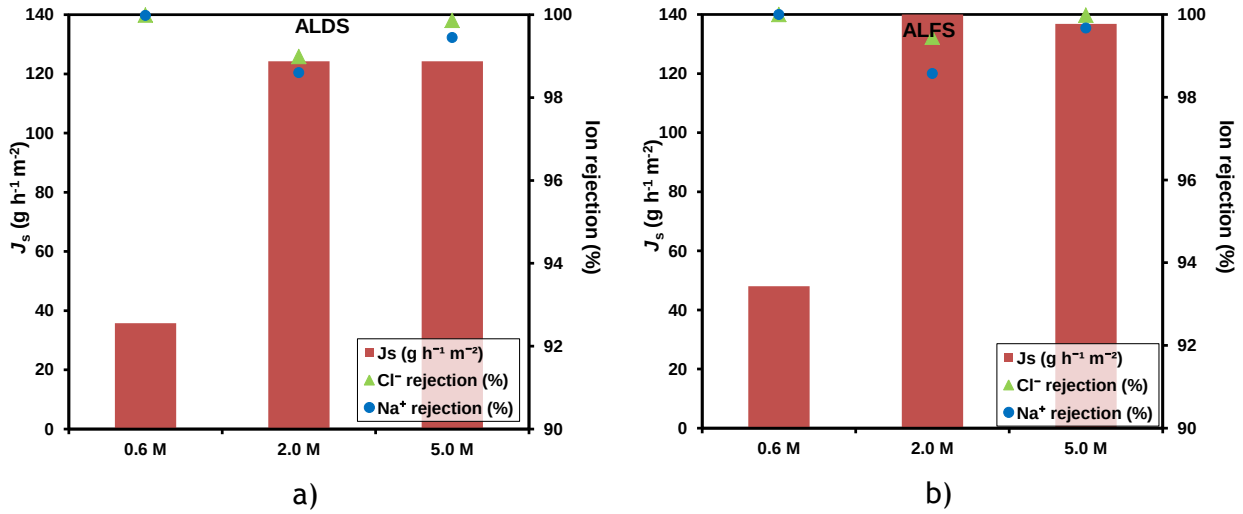

Figure 20: Reverse solute flux (J_s), Na^+ and Cl^- rejections (%) obtained in FO with different NaCl concentrations for PA-TFC: (a) ALDS and (b) ALFS configurations (W-cell; DI water as feed solution; Q_{feed} = Q_{draw} = 17 mL min^{-1}).

4.2.3 FO of the real seawater

Finally, a last experiment was carried out with the best membrane and operating conditions, namely by using a real seawater sample and NaCl 5.0 M as feed and draw solutions, respectively (Figure 21). Under these conditions, PA-TFC was active in FO, although some decrease of the water flux was observed over time with seawater, which could be due to the membrane fouling since this behavior was not observed when DI water was used as feed solution. In the experiment with seawater, the ALDS orientation is clearly the most recommended to obtain the best performance.

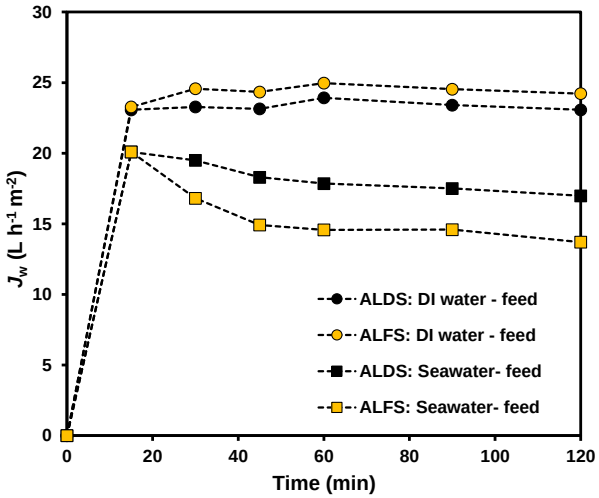

Figure 21: Water flux obtained in FO with seawater and 5.0 M NaCl as feed and draw solutions, respectively, for PA-TFC (W-Cell; Q_{feed} = Q_{draw} = 17 mL min^{-1}).

Therefore, the seawater desalination driven by FO was performed in optimized conditions, although future studies are still needed to enhance the reverse solute flux and the membrane lifetime.

5 Conclusions

TFC membranes were prepared by interfacial polymerization method using four different hydrophilic commercial membranes (CA, MCE, PES and PA) as supports. All membranes presented a symmetric structure with exception of PES and PES-TFC. In all cases, the polyamide layer was homogenously deposited on the corresponding support, producing a decrease of the hydrophilicity and porosity.

TFC membranes were tested in FO with DI water and 0.6 M NaCl, as feed and draw solutions, respectively, generally presenting better performances in ALDS configuration than in ALFS. The PA-TFC membrane showed the best performance in FO (i.e., highest water flux, moderate solute reverse flux), with a J_w = 10.7 L h^{-1} m^{-2}, J_s = 36 g h^{-1} m^{-2} and 99.98 % of ions rejection.

Different operating conditions were studied with the most active membrane (PA-TFC), and the highest performance was obtained by using draw and feed flow rates of 17 mL min^{-1}, a W-cell configuration, ALDS orientation, and a 5.0 M concentration of NaCl as draw solution. In these optimized conditions, a J_w = 23.7 L h^{-1} m^{-2}, J_s = 124 g h^{-1} m^{-2} and 99.36 % of ions rejection were reached.

Finally, seawater desalination was demonstrated to take place by the FO process under the membrane and operating conditions optimized along this MSc Thesis.

6 Future work

The next important step in the FO process will be to recover the water from diluted draw solution in order to produce fresh water by the FO process. FO can be coupled with other desalination processes, like membrane distillation (MD), leading to a hybrid FO-MD system, which separates water, regenerates the draw solute and avoids the organic fouling and/or mineral scaling that are detrimental for MD.

Since the operating conditions were optimized for TFC membranes on commercial supports, different lab-prepared supports could be developed in order to increase the water flux and the solute rejection. These new home-made membranes should present a low thickness and a high porosity, i.e., a low structural parameter, which enhances the membrane performance.

7 References

[1] S. Atkinson, World's largest desalination plant begins operating in Israel, Membrane Technology 2005 (2005) 9-10.

[2] T.Y. Cath, A.E. Childress, M. Elimelech, Forward osmosis: Principles, applications, and recent developments, Journal of Membrane Science 281 (2006) 70-87.

[3] I.C. Karagiannis, P.G. Soldatos, Water desalination cost literature: review and assessment, Desalination 223 (2008) 448-456.

[4] C. Charcosset, A review of membrane processes and renewable energies for desalination, Desalination 245 (2009) 214-231.

[5] T.-S. Chung, S. Zhang, K.Y. Wang, J. Su, M.M. Ling, Forward osmosis processes: Yesterday, today and tomorrow, Desalination 287 (2012) 78-81.

[6] S. Zhao, L. Zou, C.Y. Tang, D. Mulcahy, Recent developments in forward osmosis: Opportunities and challenges, Journal of Membrane Science 396 (2012) 1-21.

[7] J.J. Qin, W.C.L. Lay, K.A. Kekre, Recent developments and future challenges of forward osmosis for desalination: A review, Desalination and Water Treatment 39 (2012) 123-136.

[8] G. Han, T.-S. Chung, M. Toriida, S. Tamai, Thin-film composite forward osmosis membranes with novel hydrophilic supports for desalination, Journal of Membrane Science 423–424 (2012) 543-555.

[9] R. Valladares Linares, Z. Li, S. Sarp, S.S. Bucs, G. Amy, J.S. Vrouwenvelder, Forward osmosis niches in seawater desalination and wastewater reuse, Water Research 66 (2014) 122-139.

[10] J.E. Miller, L.R. Evans, Forward Osmosis: A New Approach to Water Purification and Desalination, Sandia National Laboratories (2006).

[11] J.A. Nollet, Lecons de physique experimentable, (1748) Du fonds de H.L Guerin & L.F. Delatour, Paris.

[12] K. Popper, R.L. Merson, W.M. Camirand, Desalination by Osmosis-Reverse Osmosis Couple, Science 159 (1968) 1364-1365.

[13] R.E. Kravath, J.A. Davis, Desalination of sea water by direct osmosis, Desalination 16 (1975) 151-155.

[14] W.C.L. Lay, J. Zhang, C. Tang, R. Wang, Y. Liu, A.G. Fane, Factors affecting flux performance of forward osmosis systems, Journal of Membrane Science 394–395 (2012) 151-168.

[15] A. Sagiv, A. Zhu, P.D. Christofides, Y. Cohen, R. Semiat, Analysis of forward osmosis desalination via two-dimensional FEM model, Journal of Membrane Science 464 (2014) 161-172.

[16] A. Bennett, Desalination and water reuse: What's the future for forward osmosis?, Filtration + Separation 50 (2013) 28-34.

[17] K. Lutchmiah, A.R.D. Verliefde, K. Roest, L.C. Rietveld, E.R. Cornelissen, Forward osmosis for application in wastewater treatment: A review, Water Research 58 (2014) 179-197.

[18] C.M.P. Esteves, Membranes with nanostructured materials for water desalination and purification (2014) Master's Thesis in Chemical Engineering, University of Porto, Portugal.

[19] S.J. Bates, Osmotic pressure and concentration in solutions of electrolytes, and the calculation of the degree of ionization, Journal of the American Chemical Society 37 (1915) 1421-1445.

[20] Q. Ge, M. Ling, T.-S. Chung, Draw solutions for forward osmosis processes: Developments, challenges, and prospects for the future, Journal of Membrane Science 442 (2013) 225-237.

[21] S. Phuntsho, S. Sahebi, T. Majeed, F. Lotfi, J.E. Kim, H.K. Shon, Assessing the major factors affecting the performances of forward osmosis and its implications on the desalination process, Chemical Engineering Journal 231 (2013) 484-496.

[22] S. Phuntsho, S. Vigneswaran, J. Kandasamy, S. Hong, S. Lee, H.K. Shon, Influence of temperature and temperature difference in the performance of forward osmosis desalination process, Journal of Membrane Science 415–416 (2012) 734-744.

[23] M.I.G. Monteiro, Forward osmosis membranes tailored by hydrogel coatings (2012) Master's Thesis Chemical and Biochemical Enginering, Universidade Nova de Lisboa, Portugal.

[24] Y. Oh, S. Lee, M. Elimelech, S. Lee, S. Hong, Effect of hydraulic pressure and membrane orientation on water flux and reverse solute flux in pressure assisted osmosis, Journal of Membrane Science 465 (2014) 159-166.

[25] B.D. Coday, P. Xu, E.G. Beaudry, J. Herron, K. Lampi, N.T. Hancock, T.Y. Cath, The sweet spot of forward osmosis: Treatment of produced water, drilling wastewater, and other complex and difficult liquid streams, Desalination 333 (2014) 23-35.

[26] L. Liu, M. Wang, D. Wang, C. Gao, Current Patents of Forward Osmosis Membrane Process, Recent Patents on Chemical Engineering 2 (2009) 76-82.

[27] Q. Ge, J. Su, G.L. Amy, T.-S. Chung, Exploration of polyelectrolytes as draw solutes in forward osmosis processes, Water Research 46 (2012) 1318-1326.

[28] S.L.L.T.E.K.J. Freiman, Effect of porous support fabric on osmosis through a Loeb–Sourirajan type asymmetric membrane, Journal of Membrane Science 129 (1997) 243-249.

[29] R.W.B. K.L. Lee, H.K. Lonsdale, Membranes for power generation by pressure-retarded osmosis, Journal of Membrane Science 8 (1981) 141-171.

[30] S.L. G.D. Mehta, Internal polarization in the porous substructure of a semi-permeable membrane under pressure-retarded osmosis, Journal of Membrane Science 4 (1978) 261.

[31] J.R. McCutcheon, R.L. McGinnis, M. Elimelech, A novel ammonia—carbon dioxide forward (direct) osmosis desalination process, Desalination 174 (2005) 1-11.

[32] S. Lee, C. Boo, M. Elimelech, S. Hong, Comparison of fouling behavior in forward osmosis (FO) and reverse osmosis (RO), Journal of Membrane Science 365 (2010) 34-39.

[33] Y. Gao, Y.-N. Wang, W. Li, C.Y. Tang, Characterization of internal and external concentration polarizations during forward osmosis processes, Desalination 338 (2014) 65-73.

[34] S. Loeb, The Loeb-Sourirajan Membrane: How It Came About, American Chemical Society 153 (1981) 1-9.

[35] J.R. McCutcheon, Elimelech, M., Influence of membrane support layer hydrophobicity on water flux in osmotically driven membrane processes, Journal of Membrane Science 318(1-2) (2008) 458-466.

[36] E.R. Cornelissen, D. Harmsen, K.F. de Korte, C.J. Ruiken, J.-J. Qin, H. Oo, L.P. Wessels, Membrane fouling and process performance of forward osmosis membranes on activated sludge, Journal of Membrane Science 319 (2008) 158-168.

[37] M. Sairam, E. Sereewatthanawut, K. Li, A. Bismarck, A.G. Livingston, Method for the preparation of cellulose acetate flat sheet composite membranes for forward osmosis—Desalination using MgSO4 draw solution, Desalination 273 (2011) 299-307.

[38] Q. Yang, K.Y. Wang, T.-S. Chung, Dual-Layer Hollow Fibers with Enhanced Flux As Novel Forward Osmosis Membranes for Water Production, Environmental Science & Technology 43 (2009) 2800-2805.

[39] J. Su, Q. Yang, J.F. Teo, T.-S. Chung, Cellulose acetate nanofiltration hollow fiber membranes for forward osmosis processes, Journal of Membrane Science 355 (2010) 36-44.

[40] Q. Saren, C.Q. Qiu, C.Y. Tang, Synthesis and Characterization of Novel Forward Osmosis Membranes based on Layer-by-Layer Assembly, Environmental Science & Technology 45 (2011) 5201-5208.

[41] R. Wang, L. Shi, C.Y. Tang, S. Chou, C. Qiu, A.G. Fane, Characterization of novel forward osmosis hollow fiber membranes, Journal of Membrane Science 355 (2010) 158-167.

[42] L. Setiawan, R. Wang, K. Li, A.G. Fane, Fabrication of novel poly(amide–imide) forward osmosis hollow fiber membranes with a positively charged nanofiltration-like selective layer, Journal of Membrane Science 369 (2011) 196-205.

[43] C. Qiu, S. Qi, C.Y. Tang, Synthesis of high flux forward osmosis membranes by chemically crosslinked layer-by-layer polyelectrolytes, Journal of Membrane Science 381 (2011) 74-80.

[44] H.-Y. Yu, X.-C. He, L.-Q. Liu, J.-S. Gu, X.-W. Wei, Surface modification of polypropylene microporous membrane to improve its antifouling characteristics in an SMBR: N2 plasma treatment, Water Research 41 (2007) 4703-4709.

[45] N. Widjojo, T.-S. Chung, M. Weber, C. Maletzko, V. Warzelhan, The role of sulphonated polymer and macrovoid-free structure in the support layer for thin-film composite (TFC) forward osmosis (FO) membranes, Journal of Membrane Science 383 (2011) 214-223.

[46] S. Zou, Y. Gu, D. Xiao, C.Y. Tang, The role of physical and chemical parameters on forward osmosis membrane fouling during algae separation, Journal of Membrane Science 366 (2011) 356-362.

[47] K. Gerstandt, K.V. Peinemann, S.E. Skilhagen, T. Thorsen, T. Holt, Membrane processes in energy supply for an osmotic power plant, Desalination 224 (2008) 64-70.

[48] D. Emadzadeh, W.J. Lau, T. Matsuura, M. Rahbari-Sisakht, A.F. Ismail, A novel thin film composite forward osmosis membrane prepared from PSf–TiO_2 nanocomposite substrate for water desalination, Chemical Engineering Journal 237 (2014) 70-80.

[49] T.L.S. Silva, S. Morales-Torres, J.L. Figueiredo, A.M.T. Silva, Multi-walled carbon nanotube/PVDF blended membranes with sponge- and finger-like pores for direct contact membrane distillation, Desalination 357 (2015) 233-245.

[50] S. Brunauer, P.H. Emmett, E. Teller, Adsorption of gases in multimolecular layers, Journal of the American Chemical Society 60 (1938) 309-319.

[51] F. Rouquerol, J. Rouquerol, K. Sing, Adsorption by Powders and Porous Solids. Principles, Methodology and Applications, (1999) Academic Press, London.

[52] L.M. Pastrana-Martínez, S. Morales-Torres, S.K. Papageorgiou, F.K. Katsaros, G.E. Romanos, J.L. Figueiredo, J.L. Faria, P. Falaras, A.M.T. Silva, Photocatalytic behaviour of nanocarbon-TiO_2 composites and immobilization into hollow fibres, Applied Catalysis B: Environmental 142-143 (2013) 101-111.

[53] P. Pardeshi, A.A. Mungray, Synthesis, characterization and application of novel high flux FO membrane by layer-by-layer self-assembled polyelectrolyte, Journal of Membrane Science 453 (2014) 202-211.

[54] C. Kim, S. Lee, H.K. Shon, M. Elimelech, S. Hong, Boron transport in forward osmosis: Measurements, mechanisms, and comparison with reverse osmosis, Journal of Membrane Science 419–420 (2012) 42-48.

[55] C.Y. Tang, Q. She, W.C.L. Lay, R. Wang, A.G. Fane, Coupled effects of internal concentration polarization and fouling on flux behavior of forward osmosis membranes during humic acid filtration, Journal of Membrane Science 354 (2010) 123-133.

[56] J. Wei, X. Liu, C. Qiu, R. Wang, C.Y. Tang, Influence of monomer concentrations on the performance of polyamide-based thin film composite forward osmosis membranes, Journal of Membrane Science 381 (2011) 110-117.